C.P. No. 1229

C.P. No. 1229

PROCUREMENT EXECUTIVE, MINISTRY OF DEFENCE

AERONAUTICAL RESEARCH COUNCIL

CURRENT PAPERS

Design Development of an Aircraft Strut in Carbon Fibre Reinforced Plastic

by

T. A. Collings

Structures Dept., R.A.E., Farnborough

LONDON: HER MAJESTY'S STATIONERY OFFICE

1972

PRICE £1 NET

UDC 629.13.012.563 : 621-23 : 661.66-426 : 678.046

CP No.1229 *
February 1972

DESIGN DEVELOPMENT OF AN AIRCRAFT STRUT IN CARBON FIBRE REINFORCED PLASTIC

by

T. A. Collings

SUMMARY

An actuator reaction strut from the VC 10 aileron power control circuit, made from steel, has been redesigned, made and tested in carbon fibre reinforced plastic (CFRP) with aluminium alloy ends, partly to demonstrate the weight saving potential of CFRP in this type of application and partly to investigate some of the problems of jointing and load diffusion which CFRP presents.

The strut has overall axial strength and stiffness requirements in both tension and compression. All have been met with the redesigned CFRP strut with the exception of tensile stiffness, the low value of which was shown to be fundamental to the form of end attachment adopted.

This Report describes the design, fabrication and testing of the CFRP strut which weighed 43% less than the original steel component.

---

* Replaces RAE Technical Report 72032 - ARC 33853

CONTENTS

1 INTRODUCTION

Carbon fibre reinforced plastic (CFRP) has provided structural engineers and designers in the aerospace industry with a material of great potential. The combination of low density and high strength and stiffness promises very substantial structural weight savings if the novel problems of design and fabrication can be solved. The exercise described in this Report was one of a number of early experimental investigations aimed partly at demonstrating the weight savings which could be shown on paper, and partly at contributing to the solution of some of these novel problems.

A VC 10 aileron control strut was chosen for redesign for a number of reasons: the loads are highly directional and this invites the use of CFRP in the highly anisotropic form in which most weight is likely to be saved; the component was shorter than the longest carbon fibres then available (1 m); fabrication by moulding from dry fibres and resin was feasible, there being no pre-impregnated CFRP sheet or tape at that time; the problems of end design and load transfer were of general interest.

Details of the design, fabrication and testing of the CFRP strut and its end attachments are given here. The limitations of the design are discussed and suggestions for possible alternatives are given.

2 THE EXISTING STEEL STRUT

This component is one of the actuator reaction struts used on the VC 10 for reacting the aileron hinge loads, and is illustrated in Figs.1 and 2. The strut is made of a T45 steel tube of 38.1 mm outside diameter and 2 mm wall thickness, 52 cm long, pinned at each end with five SP28 steel taper pins, 6.35 mm in diameter, to a forged S107 steel end fitting incorporating a spherical bearing. The strut is pin jointed at both ends and is attached to the aircraft by means of shear pins as illustrated in Fig.3, the distance between pin centres being 67.26 cm. The geometrical shape and size of the strut are partly determined by space limitations. The strut must be capable of carrying a fully factored axial tensile load of 117.6 kN and a corresponding axial compressive load of 122.8 kN. In addition, to ensure acceptable control circuit response to pilot induced control movements, a minimum value of 70 kN/mm for both tensile and compressive stiffness is required. This design requirement on stiffness led to the original choice of steel for the main compression tube and, because of possible corrosion problems due to interaction of dissimilar metals, steel end fittings were used. The weight of the strut components are:

Tube		952 g
Two eye end fittings		1720 g
Two spherical bearings		154 g
Extras		44 g
	Total	2870 g

3 GENERAL DESIGN OF CFRP STRUT

3.1 Preliminary work

Some early work on struts made from glass reinforced plastic and designed to carry both tension and compression is reported elsewhere[1], and one of the later designs from that work is shown in Figs.4 and 5. The compression member of the strut was made from unidirectional glass fibre and a cold-setting epoxy resin system* and was manufactured by a leaky mould technique. To enable the struts to take tensile loads, an overwind of glass fibre and resin was made consolidating a steel end fitting on to each end of the compression member. To save weight, the material was machined away from the compression member section at mid-span where the tension overwind material could be expected to contribute to the compression strength. Because separate material was in general used to carry the tensile and compressive loads, this design proved excessively heavy. Moreover applying alternate tensile and compressive loads broke the bond between the end fittings and the compression member. For these reasons this type of design was not considered further in the present exercise.

3.2 Design of the main CFRP member

3.2.1 General remarks

The design conditions for the existing steel strut referred to in section 2 were used in the design of the replacement strut so that a direct comparison of weights could be made. With the experience reported in section 3.1 it was decided to design a strut that would carry both tensile and compressive loads in the same material, and a circular tube of unidirectional CFRP was chosen in view of its uniformly high second moment of area and its uncomplicated section which can be easily moulded. The tube is portrayed in detail in Fig.6.

---

* CIBA MY753 resin and HY951 hardener ∿ 6/1 parts by volume cured at room temperature.

3.2.2 Calculation of tube dimensions

The cross-sectional dimensions of the tube were calculated to give minimum outside diameter consistent with resistance to overall buckling and with the use of the minimum amount of material necessary to provide the required tensile and compressive strength and stiffness. However, since the ultimate compressive strength of unidirectional CFRP is generally less than the corresponding ultimate tensile strength, and since the compressive load carrying requirement is slightly greater than the tensile, tensile strength is not a critical design case. Moreover, it has been shown[2] that tensile elastic modulus is slightly greater than the equivalent flexural modulus, so if the latter is taken as the average of tensile and compressive values, compressive modulus must be less than tensile. Since the tensile and compressive stiffness requirements are equal, it follows again that tensile stiffness is not a design case. Attention can therefore be concentrated on designing the tube to resist the maximum compressive load from the points of view of strength, stiffness and overall buckling.

Let the tube have internal and external radii r and R respectively, cross-sectional area A, length L between pin joints, and let the maximum compressive load P produce a decrease in length δL. Then if E is the compressive elastic modulus and I the second moment of area of the tube, Euler buckling will not occur if

$$I \geqslant \frac{PL^2}{E\pi^2} \quad . \tag{1}$$

Again, if λ is the required axial stiffness the minimum acceptable value of A is given by

$$A = \frac{\lambda L}{E} \quad . \tag{2}$$

If σ is the ultimate compressive strength, then the minimum value of A to carry the load P is given by

$$A = \frac{P}{\sigma} \quad . \tag{3}$$

The numerical values of L, P and λ are known. The values of σ and E depend on the type and fibre volume fraction of the carbon used in the tube.

Because preliminary calculations showed that compressive stiffness rather than strength was likely to be the dominant consideration, Type I fibre was chosen at a fibre volume fraction v_f of 0.50, which was about the highest which could be moulded easily. A typical fibre tensile elastic modulus for this material is 414 GN/m^2; using this figure and the results of Ref.2, and assuming flexural composite modulus to be the average of the tensile and compressive figures, E was calculated to be 163 GN/m^2 and this figure was used in the tube design. For the same composite material 448 MN/m^2 is a typical value for σ and this also was used for design.

Minimum values of I and A were then calculated from equations (1) to (3) and found to be,

$$I = 34590 \text{ mm}^4$$

$$A = 290.3 \text{ mm}^2 \quad .$$

It is evident from these calculations that the critical design constraints are governed by equations (1) and (2); that is the second moment of area required to prevent buckling and the area required to give adequate linear compressive stiffness. Now since $I = \frac{\pi}{4}(R^4 - r^4)$ and $A = \pi(R^2 - r^2)$, we have

$$r = \sqrt{\frac{2I}{A} - \frac{A}{2\pi}} \quad .$$

Substitution of the values of I and A from equations (1) and (2) respectively gives the minimum internal tube radius

$$r = 13.87 \text{ mm}$$

and hence the minimum external tube radius

$$R = 16.84 \text{ mm} \quad .$$

These dimensions were rounded up to the nearest practical Imperial sizes, giving the following values which were used in the experimental work:

$$r = 14.29 \text{ mm}$$

$$R = 17.46 \text{ mm} \quad .$$

3.2.2 Calculation of tube dimensions

The cross-sectional dimensions of the tube were calculated to give minimum outside diameter consistent with resistance to overall buckling and with the use of the minimum amount of material necessary to provide the required tensile and compressive strength and stiffness. However, since the ultimate compressive strength of unidirectional CFRP is generally less than the corresponding ultimate tensile strength, and since the compressive load carrying requirement is slightly greater than the tensile, tensile strength is not a critical design case. Moreover, it has been shown[2] that tensile elastic modulus is slightly greater than the equivalent flexural modulus, so if the latter is taken as the average of tensile and compressive values, compressive modulus must be less than tensile. Since the tensile and compressive stiffness requirements are equal, it follows again that tensile stiffness is not a design case. Attention can therefore be concentrated on designing the tube to resist the maximum compressive load from the points of view of strength, stiffness and overall buckling.

Let the tube have internal and external radii r and R respectively, cross-sectional area A, length L between pin joints, and let the maximum compressive load P produce a decrease in length δL. Then if E is the compressive elastic modulus and I the second moment of area of the tube, Euler buckling will not occur if

$$I \geqslant \frac{PL^2}{E\pi^2} \quad . \tag{1}$$

Again, if λ is the required axial stiffness the minimum acceptable value of A is given by

$$A = \frac{\lambda L}{E} \quad . \tag{2}$$

If σ is the ultimate compressive strength, then the minimum value of A to carry the load P is given by

$$A = \frac{P}{\sigma} \quad . \tag{3}$$

The numerical values of L, P and λ are known. The values of σ and E depend on the type and fibre volume fraction of the carbon used in the tube.

Because preliminary calculations showed that compressive stiffness rather than strength was likely to be the dominant consideration, Type I fibre was chosen at a fibre volume fraction v_f of 0.50, which was about the highest which could be moulded easily. A typical fibre tensile elastic modulus for this material is 414 GN/m^2; using this figure and the results of Ref.2, and assuming flexural composite modulus to be the average of the tensile and compressive figures, E was calculated to be 163 GN/m^2 and this figure was used in the tube design. For the same composite material 448 MN/m^2 is a typical value for σ and this also was used for design.

Minimum values of I and A were then calculated from equations (1) to (3) and found to be,

$$I = 34590 \text{ mm}^4$$

$$A = 290.3 \text{ mm}^2 \quad .$$

It is evident from these calculations that the critical design constraints are governed by equations (1) and (2); that is the second moment of area required to prevent buckling and the area required to give adequate linear compressive stiffness. Now since $I = \frac{\pi}{4}(R^4 - r^4)$ and $A = \pi(R^2 - r^2)$, we have

$$r = \sqrt{\frac{2I}{A} - \frac{A}{2\pi}} \quad .$$

Substitution of the values of I and A from equations (1) and (2) respectively gives the minimum internal tube radius

$$r = 13.87 \text{ mm}$$

and hence the minimum external tube radius

$$R = 16.84 \text{ mm} \quad .$$

These dimensions were rounded up to the nearest practical Imperial sizes, giving the following values which were used in the experimental work:

$$r = 14.29 \text{ mm}$$

$$R = 17.46 \text{ mm} \quad .$$

The similarity between the dimensions of the CFRP tube and the existing steel tube is not unexpected, as both tubes are designed to the same stiffness constraints and both materials exhibit similar moduli.

3.3 End fitting design

The end fitting has to fulfil a dual purpose. Firstly it has to provide attachment to the existing reaction points and secondly it must be capable of transferring load into the CFRP tube.

End fitting designs that lend themselves to tubes are the CFRP metal multi-shim joint and both convergent and divergent wedges. The multi-shim joint, which consists of alternate thin layers of metal and CFRP, is limited only by the bond strength between the layers, but it is extremely complicated to fabricate as it requires close tolerance shim manufacture and skilful assembly. Both convergent and divergent wedges rely as the name implies on a mechanical wedging action to transfer load. The convergent wedge has the advantage of a less bulky end, but is restricted to large tube mouldings using the wet lay-up moulding technique because of the difficulty of mandrel removal. The divergent wedge although suffering a bulky end is readily fabricated by the wet lay-up moulding technique and was therefore chosen as the end fitting to be used in this exercise. The choice of the angle of divergence of the tube end was a compromise based on the one hand on the loss of axial load carrying capacity due both to a change in fibre alignment and to bending at the change of section, and on the other on the high hoop stresses developed due to the wedge action, which increase with a decrease in wedge angle. This resulted in the choice of a 20 degree included angle wedge.

The end fitting assembly which is illustrated in Figs.7 and 8 comprises an eye end, a clamping ring, a tension plug, and a split collet; these were machined from extruded bar of L65 aluminium alloy, chosen for its good ultimate strength to weight ratio. Because the end fittings were required for testing several strut assemblies up to ultimate design conditions, they were so designed that the 0.1% proof stress was not exceeded. The eye end was made similar to that used on the original strut and was designed to the axial loading conditions referred to in section 2 using a standard lug design technique[3]. Integral with the eye end is the tension plug which supports the tube end against radial crushing by compressive hoop loads when the strut assembly is loaded in tension. The eye end is attached to a clamping ring by means of a fine screw thread. This clamps the eye end to the tube mechanically and provides the means of transferring the tensile axial load from one to the other. Note that the clamping ring is subjected to both axial and hoop tensile loads. To facilitate the clamping of the tube end by the clamping ring, a split collet is provided. Compression loads are taken on the end face of the tube through direct contact with the eye end. The tension plug, split collet and clamping ring provide end support to the CFRP. Figs.9 and 10 show the action of the end fitting under both loading conditions.

The axial stiffness λ_T of the strut assembly can be calculated from the following equation

$$\lambda_T = \frac{1}{\sum_{i=1}^{i=n} \frac{1}{\lambda_i}} \quad , \qquad (4)$$

where n is the number of components contributing to the stiffness of the strut assembly and λ_i is the stiffness of the ith component. In the tensile case the components contributing to the overall stiffness are the CFRP tube, the clamping rings and the eye ends. In compression the components are the CFRP tube and the eye ends. The stiffnesses of the components can be calculated from equation (2) and are as follows;

CFRP tube	163 kN/mm
Eye end	580 kN/mm
Clamping ring	2170 kN/mm .

The tensile and compressive stiffnesses of the strut assembly can be calculated using equation (4), and are 104 kN/mm and 95.3 kN/mm respectively.

4 CFRP STRUT MODEL ONE

4.1 Strut fabrication

The main CFRP member was fabricated by a wet lay-up process in which the flow of excess resin out of the moulds ends assists in aligning the fibres. The mould is shown in Figs.11 and 12. Half the weighed amount of type I carbon fibre (cut from metre length untreated Morganite material) together with excess resin* was layered in the lower half of the mould with the fibres parallel to the tube axis. After coating with resin the mandrel was aligned in the mould

---

* SHELL 828 resin, MNA and benzyl dimethylamine ∿ 100/85/1 parts by weight.

and the remaining half of the fibre and resin layered over the mandrel. The upper half of the mould was then positioned and the whole assembly placed in a hot press at 100°C and allowed to soak at this temperature until the viscosity of the resin was such that it readily flowed from the ends of the mould. Using a pressure of approximately 345 N/m^2, the mould was closed allowing all excess resin to flow out of the mould ends. The mould was then pressed to stops and the component cured *in situ* for one hour at 100°C, followed by a post cure of 24 hours at 120°C in an air circulating oven.

This fabrication process produced a tube with divergent ends which when trimmed conformed to the dimensions shown in Fig.6.

The fibre volume fraction was determined from the weight and density of fibre used and the volume of the tube. A figure of 0.50 was aimed at, but subsequent accurate fibre density measurements showed the value to be 0.48 and all subsequent tubes were made to this figure unless otherwise stated.

The weights of the CFRP strut and the aluminium alloy end components were;

CFRP tube	260 g
Two split collets	82 g
Two eye ends and two tension plugs	824 g
Two clamping rings	410 g
Total	1576 g

4.2 Tensile test

The assembled strut shown in Fig.13 was tested in tension between pin joints in an Avery testing machine. Failure occurred in the end fitting through circumferential crushing of the CFRP tube end by the compressive hoop stresses produced by the end fittings. This caused a shrinkage in the tube end section, and subsequent extrusion of the tube from between the split collet and tension plug. The failing load was 26.6 kN.

5 CFRP STRUT MODEL TWO

5.1 Modification of strut design

Two significant changes were made in the design and fabrication of this model. Firstly the fibre was surface treated by oxidation[4] in air at 550°C to a weight loss of at least 0.67% (the fibre used in this strut was made up from batches of fibre whose oxidised weight loss ranged between 0.67% and 1.2%). Secondly the end fittings were modified by separating the tension plug from the eye end and securing it to the CFRP tube with adhesive (3M's EC2216). This allowed the tension plug to move axially with the CFRP tube, preventing radial collapse and extrusion of the tube end. Surface preparation of the tension plug prior to glueing consisted of mechanical cleaning using a fine emery paper, followed by a surface preparation process using chromium trioxide to Specification DTD 915B. The CFRP tube surface was prepared by mechanical cleaning using a fine emery paper followed by washing in distilled water and finally drying in an air circulating oven.

To aid alignment of the tube and end fittings a central spigot was added to the eye end, Figs.14 and 15 show the modified end fittings and their assembly.

5.2 Tensile tests

The strut assembly designated 2/I, with split collets assembled dry, was tested in tension as before and failed at 37.9 kN. Failure occurred at the change of section at the tube end. Subsequent examination of this failure showed that the split collets were not fitting correctly around the tube at the change of section and were consequently causing a stress concentration and surface fibre damage. To overcome this, subsequent struts were assembled with split collets that had been given a generous radius at the change of section, and to allow for fitting errors they were secured with adhesive. The adhesive and surface preparations used were the same as for the tension plug referred to in section 5.1. Three further struts designated 2/II, 2/III and 2/IV were assembled using the modified split collet and then tested in tension as before. Failure of strut 2/II, shown in Fig.16, began at the end fitting at a load of 94.7 kN. Struts 2/III and 2/IV both failed in tension remote from the ends at 85.7 kN and 67.8 kN respectively. Figs.17 and 18 show the failed tubes.

Because the failures of the last two struts were apparently uninfluenced by the ends, the fibre stress at failure should have approached the fibre ultimate tensile strength (1434 MN/m^2). It was in fact substantially lower in both cases (568 MN/m^2 and 450 MN/m^2 respectively). This led to a separate investigation, reported elsewhere[5], which showed that the fibre surface treatment described in section 5.1 had substantially reduced the fibre ultimate tensile strength. The treatment was therefore changed from model 3 onwards and this is detailed in section 6.1.

5.3 Compression tests

In order to provide direct information on the ultimate compressive strength of the CFRP tubes for comparison with the design figure, several specimens were cut from a moulded CFRP tube and tested. They consisted of tube sections 102 mm long whose ends were cast in an epoxy resin* to give lateral support to the fibre ends. To ensure true axial loading of the specimens the cast end faces were machined square with the tube axis and the tests were carried out between the parallel compression platens of an Avery testing machine. One specimen with an end fitting assembled was also tested in compression to determine the effect, if any, on the compression strength of the CFRP tube.

The results and modes of failure are listed in Table 1. Figs.19 and 20 show the compression specimen and failed specimens respectively. The four tube section specimens gave a mean composite compression strength of 458 MN/m^2 which compares closely with the figure of 448 MN/m^2 used for design (see section 3.2.2). The tube cross-sectional area was, however, larger than the minimum design value in order to use practical Imperial sizes, and for the actual tube the maximum compressive design load corresponds to a stress of only 390 MN/m^2. The composite failing stress of the end fitting assembly of 390 MN/m^2 shows that this end fitting is just adequate for these design conditions.

A complete strut assembly with both tension plug and split collet secured with adhesive was tested in compression between pin joints in an Avery testing machine. Failure occurred in about 30 s at a load of 108 kN approximately one third of the way along the length of the CFRP tube. Fig.21 shows the failed specimen. The compression strength of 344 MN/m^2 obtained from this test is rather lower than the figure of 390 MN/m^2 for a single end and may have been influenced by some misalignment of the end fittings.

6 CFRP STRUT MODEL THREE

6.1 Modification of strut design

Several changes were made to the design as the result of experience.

Fibre surface treatment was changed to a wet oxidation process using sodium hypochlorite[5]. This gave improved composite shear strength without

---

* CIBA MY753 resin and HY951 hardener ∿ 6/1 parts by volume cured at room temperature.

degrading the fibre tensile strength. The fibre used for this strut and subsequent struts was a Morganite fibre whose tensile strength was 2040 MN/m^2.

Failures were still occurring at the ends so, to reduce stress concentration effects due to the abrupt change of section near the end of the CFRP tube, the shape was modified as shown in Fig.22.

To give some arbitrary transverse and torsional strength and better handling characteristics to the CFRP tube, a thin inner core tube was provided; this was helically wound onto a steel mandrel in surface treated type II fibre two tows thick to the pattern shown in Fig.23 using the filament winding machine[6] shown in Fig.24. Fabrication was then continued as described in section 4.1 giving unidirectional CFRP over the core tube. The overall fibre volume fraction in the tube section was 0.504.

Modification to the end fittings consisted of changing the design conditions from proof to ultimate figures and the inclusion of a spherical bearing similar to that used on the original strut. This bearing gives a full three degrees of freedom against unwanted induced bending and twisting loads. The split collet and tension plug were modified to suit the new shape of the tube ends. Figs.25 to 27 show respectively the modified end fittings, details of the eye end, and the split collet and tension plug.

Redesign of the eye end reduced the amount of aluminium alloy used, but spherical bearings added additional weight. Each redesigned eye end weighed 450 g giving a strut assembly weight of 1740 g.

6.2 Tensile tests

A strut assembly incorporating the new modifications was tested in tension and failed in the end fitting at a level of 113 kN due to a bearing failure in the split collet and clamping ring. Subsequent examination indicated that there was a lack of fit between the tapers of the split collet and the clamping ring so that only a fraction of the theoretical load bearing area was in contact. This lack of fit caused distortions in both components and was remedied by machining subsequent split collets after assembly, giving concentricity with the tube's axis and positive mating with the clamping ring.

A second strut, modified in this way, was assembled and tested, giving a failing load of 116.6 kN. Failure in this case was initiated by transverse compressive[7] failure of the CFRP inside the end fitting approximately 15 mm from the end of the tube, propagating around 85% of the tube's circumference.

This was followed by longitudinal shearing of the CFRP parallel to the tube axis as far as the change of tube section, where the remaining 15% failed in tension. Fig.28 shows the failed specimen.

An approximate stress analysis of the tube end has shown that compressive hoop stresses of about 480 MN/m^2 would occur at this latest tensile failing load. This agrees quite well with transverse compression strength tests[7] carried out on specimens made from the same fibre and resin system, and subjected to similar constraint, which gave ultimate failing strengths of 517 MN/m^2 and 603 MN/m^2 corresponding to fibre volume fractions of 0.4 and 0.5 respectively.

6.3 Compression test

A strut assembly with all modifications was loaded in compression and failure occurred at the end fitting at a load of 117 kN, giving a composite compressive stress at failure of 372 MN/m^2. This was not significantly better than strut two and still below the design stress of 390 MN/m^2. From the appearance of the strut, shown in Fig.29, failure may have been caused by a lack of pre-tightening of the clamping ring, so that under a compressive load some axial settlement in the tube end left the tube end unsupported except for the split collet.

7 CFRP STRUT MODEL FOUR

7.1 Modification of strut design

To finalise the design of the end attachment the clamping ring was redesigned in an aluminium alloy CFRP material combination. This consisted of an aluminium alloy L65 screwed ring designed to take the tensile axial loads, over which a continuous type II carbon fibre with epoxy resin* was circumferentially wound. This overwind (v_f = 0.50) was finally machined to an appropriate diameter and shape to take the tensile hoop stresses in an efficient manner. The maximum hoop stresses developed in the clamping ring were calculated to be 472 MN/m^2 at the tube end and 692 MN/m^2 at a point 19 mm from the tube end. This modification resulted in a weight saving on each clamping ring of 50 g, giving a 25 per cent weight reduction on the original clamping ring. Fig.30 illustrates in detail the new clamping ring and Fig.31 the finalised end fitting components.

---

* Shell 828 resin, MNA and benzyl dimethylamine $\sim$ 100/85/1 parts by weight, cured at 100°C for 1 hour, post cured at 120°C for 24 hours.

Fabrication of the CFRP tube was carried out as referred to in section 6.1 using the same type I and type II carbon fibre but with an increase in volume fraction of the type I carbon from 0.48 to 0.5, making the total volume fraction of carbon in the tube 0.524.

The weight of the final CFRP strut components were:

CFRP tube	260 g
Two split collets	82 g
Two eye ends	900 g
Two tension plugs	87 g
Two clamping rings	308 g
Total	1637 g

7.2 Tensile tests

7.2.1 Strength test

A strut assembly made to the final design, shown in Fig.32, was tested in tension and failed in the end fitting at a load of 117.6 kN at which the fibre stress was 770 MN/m^2. As before, failure was caused by a transverse compression failure of the CFRP inside the end fitting, this time approximately 8 mm from the end of the tube, followed by longitudinal shearing of the CFRP. Fig.33 shows the failed specimen. The tensile strength so measured satisfied the axial tensile loading requirement, but tensile tests[5] of CFRP specimens made from the same material as the tube have shown that a fibre strength of 1836 MN/m^2 can be achieved, so that the efficiency of the end in tension is only about 41%. The limit is set by the transverse compressive strength of the CFRP. The transverse compressive stresses may be reduced somewhat by changing the rate of divergence of the tube end, but there does not appear to be much scope for improving tensile efficiency with this type of end design.

7.2.2 Tube modulus measurement

The tensile elastic modulus of the CFRP tube was measured by a strain gauge technique. A foil strain gauge* was secured with adhesive** to the

---

* Saunders Roe batch 1843, 25.4 mm long, 100 ohm resistance and gauge factor 2.12.

** CIBA MY753 resin and HY951 hardener ∿ 6/1 parts by volume, cured at room temperature.

outside wall of the CFRP tube of a strut assembly, and aligned parallel with the tube axis as shown in Fig.34. A digital voltmeter was used for measuring the bridge voltage and also the output of the strain gauge, using a conventional Wheatstone bridge network. The strut assembly was loaded in tension between pin joints in an Avery test machine in load increments of 10 kN from 10 kN to 60 kN, the corresponding strain being recorded at each load. Fig.35 shows the load/strain curve plotted from the test results. The tensile elastic modulus calculated from these results was 255 GN/m^2, which was in good agreement with the figure of 234 GN/m^2 derived from the fibre modulus and the law of mixtures.

7.2.3 Stiffness measurement

The tensile stiffness of the strut assembly is the load required to increase the length between loading pins by one unit of length. Direct measurement of this extension between the loading pins is not practical however because of pin deflections suffered under load. Measurements were therefore taken between the side pins, shown in Fig.36 which were secured to each eye fitting normal to the strut and pin axes, and in line with the pin joint centres.

To measure the tensile stiffness the strut assembly used in section 7.2.2 was loaded in tension between pin joints, the load being applied in increments of 2.5 kN up to a maximum of 60 kN. At each load increment the corresponding increase in length was measured using a telescopic tube and displacement transducer (linearly variable differential transformer) mounted between the side pins, the voltage output of the transducer being measured with a digital voltmeter. Fig.37 shows the load extension curve for the loading and unloading cycle. The slope of the linear portion of the curve on the loading cycle gives the stiffness of the strut assembly as 20.4 kN/mm.

Although the value obtained during a single loading cycle must be treated with caution, the result obtained falls so far below specification as not to merit an investigation involving repeated loading which would at that time have been inconvenient. It is, however, of interest to compare this value with a single theoretical estimate calculated in the manner described in section 3.3.

Because of the modifications to the strut components the tensile stiffness of each finalised component was re-estimated using equation (2) giving the following values:

CFRP tube	163 kN/mm
Eye end	490 kN/mm
Clamping ring	1420 kN/mm

The tensile stiffness of the finalised strut assembly determined from equation (4) is then 86 kN/mm.

The measured tensile stiffness is very much lower than that calculated, and this is clearly due to the method of end attachment. The qualitative explanation is as follows. It has already been shown that axial tensile loads generate substantial radial stresses in the divergent wedge end of the CFRP tube; indeed, these same stresses eventually initiate overall tensile failure. Because the transverse compressive modulus of the tube is low (about 7 GN/m^2), these stresses lead to substantial radial elastic deformations. These in turn lead to axial movement in the wedge, the magnitude of which is aggravated by the relatively shallow wedge angle. It is these strains which explain the difference between the measured and calculated overall stiffness.

The marked hysterisis effect evident in Fig.37 arises largely in the end fitting, in particular from the friction between the tube end and the clamping ring during unloading.

7.3 Compression tests

7.3.1 Strength test

A strut assembly made to the final design (Fig.32) was tested in compression. Failure occurred in about 30 s away from the end fitting at a load of 141.5 kN, corresponding to a composite compressive stress of 450 MN/m^2. This more than satisfied the compressive load requirement of 122.8 kN. Fig.38 shows the failed specimen.

7.3.2 Tube modulus measurement

The compressive modulus of the CFRP tube was measured using the same method and strut assembly as used for the tensile modulus described in section 7.2.2. Fig.39 shows the load/strain curve plotted from the test results. The compressive elastic modulus calculated from these results was 247 GN/m^2, while the modulus estimated in section 3.2.2 using the results of Ref.2 was only 163 GN/m^2. The tensile modulus of the fibre used was 10% higher than the figure used in the design calculations, but nevertheless the assumptions used in section 3.2.2 were evidently unduly conservative as the compressive modulus measured here is little different from the tensile figure.

7.3.3 Stiffness measurement

The overall compressive stiffness was measured using the method described in section 7.2.3 for the measurement of tensile stiffness. Fig.40 shows the load extension (-ve) curve for the loading and unloading cycle. The slope of the linear portion of the curve on the loading cycle gives the stiffness of the strut assembly as 88.5 kN/mm. The theoretical stiffness calculated from equation (4) in section 3.3, and using the re-calculated stiffness for the strut components referred to in section 7.2.3, was 98 kN/mm. This agrees adequately with the measured value.

The measured value satisfies the design tensile stiffness value of 70 kN/mm (section 2). The close agreement between measured and calculated values in this case highlights the difference in stress distribution between the tensile and compressive cases. In the former load is transferred from the pin via the clamping ring and this generates high transverse compressive stresses with the results which have been described in section 7.2.3. In the latter load is transferred directly from the eye end to the ends of the tension plug, tube and split collet.

Under axial compression the strut suffers an axial strain which for increasing load is linearly proportional to the applied load (Fig.40). During unloading however the strain is far from linear and the strut exhibits a marked hysterisis. A possible explanation is that during loading the flared end of the CFRP tube is subjected to stresses which cause a change in the local tube diameter. This in turn causes a significant amount of relative movement between the clamping ring and the tapered split collet. During the unloading cycle relative movement between the two components is inhibited by friction forces and such movement does not occur until the frictional forces are overcome, resulting in apparent hysterisis.

It can be seen that the deformation of the tube end has a less effect on overall hysterisis in compression than in tension. As previously described (section 7.2.3), hysterisis in tension is largely caused by the wedge action.

8 DISCUSSION AND CONCLUSIONS

The final CFRP strut (model 4) weighed 43% less than the existing steel component, and the quantitative results are summarised in Table 2.

Both the strength and stiffness of the complete strut in compression were satisfactory. The values of compressive strength assumed in the original design, the values obtained from small tube sections and the value obtained from a complete model 4 strut all agreed closely. Strut failures in compression showed no sign of overall buckling, did not appear to be influenced in any way by the ends, and the design compressive load was achieved comfortably. The CFRP tube compressive modulus and the overall compressive stiffness of the strut exceeded the value assumed in design and the design requirement respectively. It appears therefore that the method of design, and in particular the form of end attachment, would be satisfactory for a compression member of this kind.

The tensile results were less encouraging. The model 4 strut failed in tension at exactly the design requirement value, but the failure occurred in the end fitting at a load corresponding only to an estimated 41% of the ultimate tensile strength of the main CFRP tube. It was clearly established that the end failure was caused by the transverse compressive stress in the flared end of the CFRP tube, and an estimate of the value of this stress at failure agreed quite well with independent measurements of the transverse compressive strength of the material. The tensile modulus of the CFRP tube was slightly higher than expected, but the overall strut stiffness was well below the design requirement value. This inadequacy was shown to be a consequence of the low transverse compressive modulus of the CFRP. Under tensile loads lower than that precipitating transverse compressive failure in the CFRP flared end, the low transverse compressive modulus permits relatively large radial elastic strains which, because of the small wedge angle, lead to large corresponding axial movement within the end fitting. Both the strength and stiffness of the end fitting are therefore limited in tension by the transverse compressive performance of the CFRP. There does not appear to be a great deal of scope for improvement, either in the material properties which affect this performance or in detailed design, and this type of end design is not therefore generally suitable for a component of this kind designed to carry tensile loads. A more promising approach would seem to be an adaptation of the shim joint concept. This might take the form of a number of concentric cylindrical metal shims bonded between layers of CFRP at each end of the tube and drilled to take loading pins. An end attachment of this kind in plane form has given ultimate tensile strength efficiencies much higher than that achieved in the work reported here, and its stiffness should not be limited by the transverse properties of CFRP.

Several interesting lessons were learned during the course of the work, among them the reduction in fibre ultimate tensile strength caused by air oxidation surface treatment under certain conditions, and the importance of accurate fit of the end attachment components to avoid stress concentrations as far as possible.

Some aspects of the design were considered only partially or not at all. The provision of some torsional strength and handling integrity by means of a helically wound core was demonstrated only qualitatively, but no difficulty can be foreseen in using the technique in a real design. Fretting could clearly be a problem in the end components and was taken account of in the work reported here only by bonding the CFRP tube to the metal fittings with an adhesive to prevent surface fibre damage. Methods of protection against corrosion between the aluminium alloy end fittings and the CFRP tube were not considered and no fatigue measurements were made.

Overall, the exercise has demonstrated quantitatively the weight saving potential of CFRP in compression struts of this kind and has contributed to the solution of the difficult problems of attachment and load diffusion which the use of CFRP in highly anisotropic form presents.

Table 1

COMPRESSION STRENGTH OF SPECIMENS CUT FROM CFRP TUBE STRUT MODEL TWO

Specimen	Failing load kN	Composite compression strength MN/m^2	Remarks
1	122.6	390	Compression failure
2	147	468	Compression failure
3	142.7	454	Compression failure
4	164	522	Compression failure
5	122.6	390	Tested with end fitting Failed at end fitting

Several interesting lessons were learned during the course of the work, among them the reduction in fibre ultimate tensile strength caused by air oxidation surface treatment under certain conditions, and the importance of accurate fit of the end attachment components to avoid stress concentrations as far as possible.

Some aspects of the design were considered only partially or not at all. The provision of some torsional strength and handling integrity by means of a helically wound core was demonstrated only qualitatively, but no difficulty can be foreseen in using the technique in a real design. Fretting could clearly be a problem in the end components and was taken account of in the work reported here only by bonding the CFRP tube to the metal fittings with an adhesive to prevent surface fibre damage. Methods of protection against corrosion between the aluminium alloy end fittings and the CFRP tube were not considered and no fatigue measurements were made.

Overall, the exercise has demonstrated quantitatively the weight saving potential of CFRP in compression struts of this kind and has contributed to the solution of the difficult problems of attachment and load diffusion which the use of CFRP in highly anisotropic form presents.

Table 1

COMPRESSION STRENGTH OF SPECIMENS CUT FROM CFRP TUBE STRUT MODEL TWO

Specimen	Failing load kN	Composite compression strength MN/m^2	Remarks
1	122.6	390	Compression failure
2	147	468	Compression failure
3	142.7	454	Compression failure
4	164	522	Compression failure
5	122.6	390	Tested with end fitting Failed at end fitting

Table 2

SUMMARY OF RESULTS

		Tension				Compression			
		Load at failure (kN)	CFRP ultimate strength (MN/m^2)	CFRP modulus (GN/m^2)	Overall stiffness (kN/mm)	Load at failure (kN)	CFRP ultimate strength (MN/m^2)	CFRP modulus (GN/m^2)	Overall stiffness (kN/mm)
Model 1	Complete strut	*26.6	84						
Model 2	Tube sections					144	458		
	Single end fitting					*122.6	390		
	Complete strut 2/I	*37.9	121						
	Complete strut 2/II	*94.7	301						
	Complete strut 2/III	85.7	273						
	Complete strut 2/IV	67.8	216						
	Complete strut					108	344		
Model 3	Complete strut	*113	360						
	Complete strut	*116.6	371						
	Complete strut					117	372		
Model 4	Complete strut	*117.6	374						
	Complete strut			255	20.4				
	Complete strut					141.5	450		
	Complete strut							247	88.5
Design requirement		117.6			70	122.8			70
Value calculated using fibre properties and law of mixtures			918	234					
Value used for design							448	163	
Theoretical values					86				98

* End failure.

SYMBOLS

A	cross-sectional area of CFRP tube
E	compressive elastic modulus
I	second moment of area of the CFRP tube
L	length of strut between pin joints
n	number of components contributing to the strut assembly's linear stiffness
P	maximum compressive load
R	outside radius of CFRP tube
r	inside radius of CFRP tube
v_f	volume fraction of fibre
δL	increase or decrease in length L
λ	linear stiffness of CFRP tube
λ_i	linear stiffness of each strut component
λ_T	linear stiffness of strut assembly
σ	ultimate compressive strength

REFERENCES

No.	Author	Title, etc.
1	T.A. Collings	Compression tests on struts made from a glass fibre composite. Unpublished MOD(PE) material
2	T.A. Collings R.G. Finbow	Variation of Young's modulus with fibre volume fraction in unidirectional carbon fibre reinforced plastic. RAE Technical Report 70006 (1970)
3		The College of Aeronautics (Department of Aircraft Design) Stressing Data Sheets, September 1961
4	N.J. Wadsworth W. Watt	Some preliminary experiments on improving the bond strength between RAE carbon fibres and resin. Unpublished MOD(PE) material
5	T.A. Collings P.D. Ewins	RAE Technical Report to be published
6	T.A. Collings	Unpublished MOD(PE) material
7	T.A. Collings	RAE Technical Report to be published

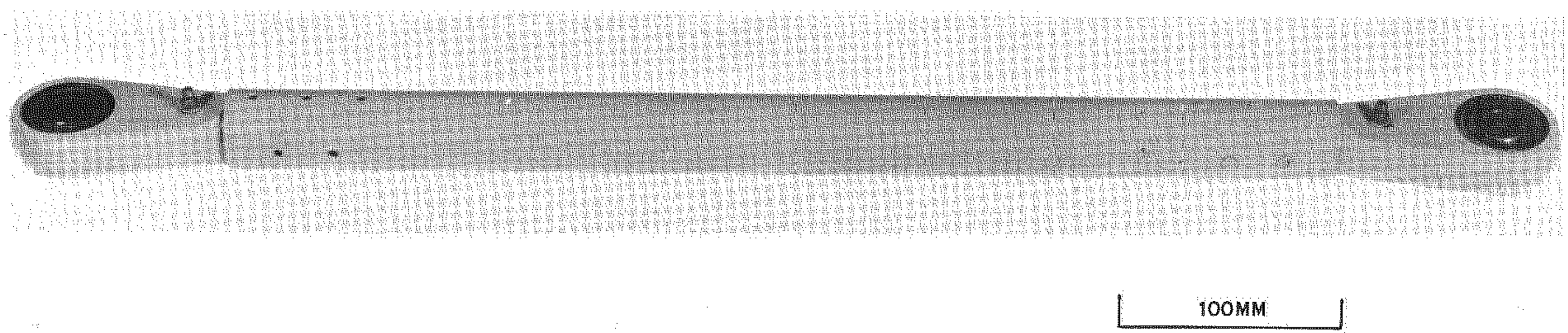

Fig.1 Steel strut

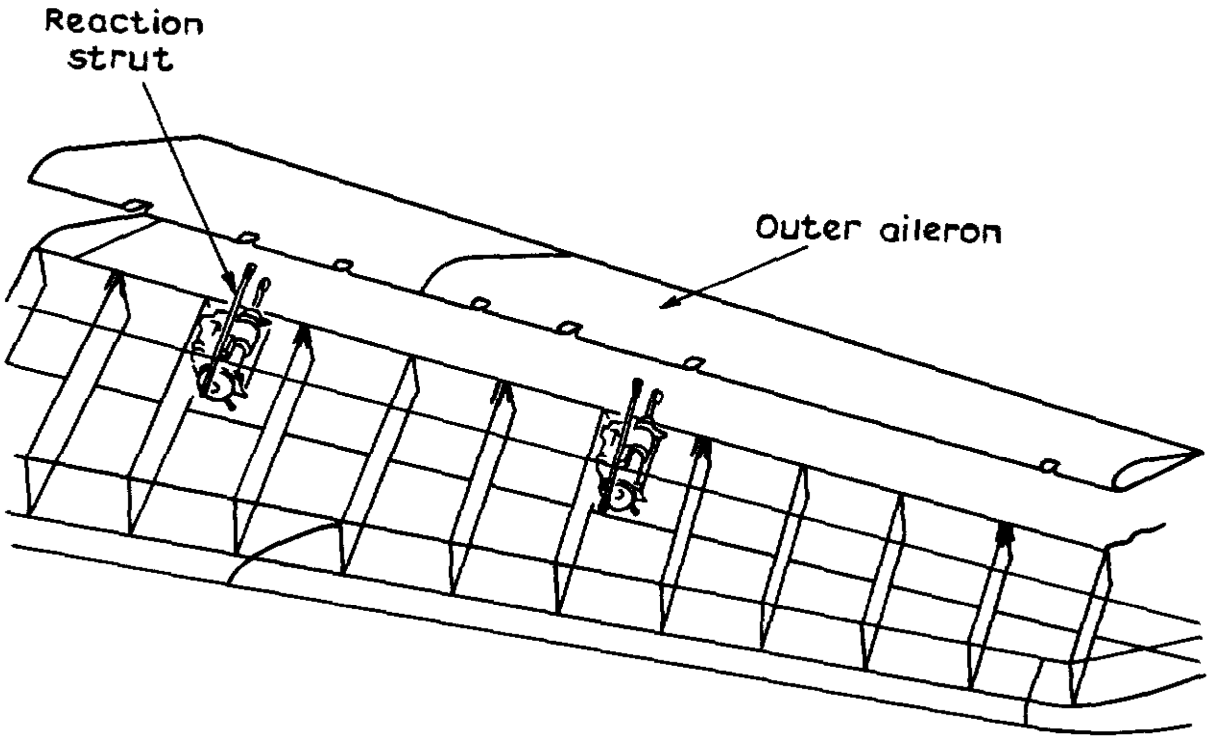

Fig.2 Position of strut in aircraft

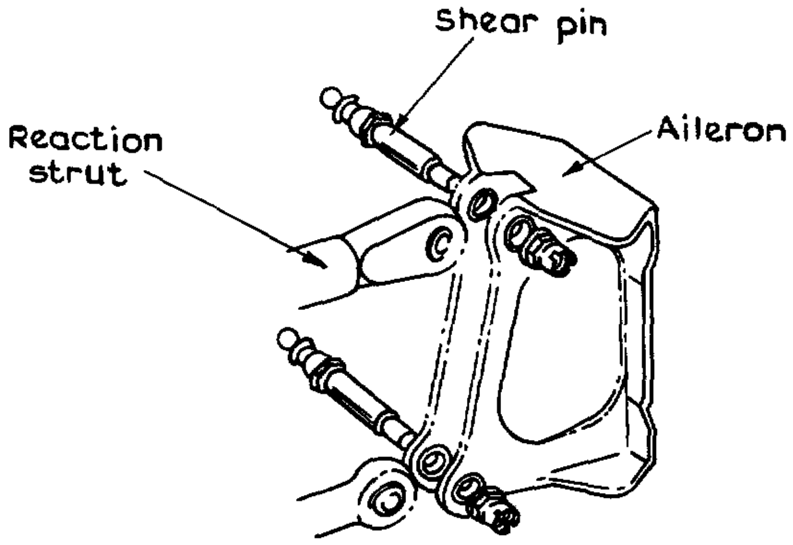

Fig.3 Attachment of strut to aircraft

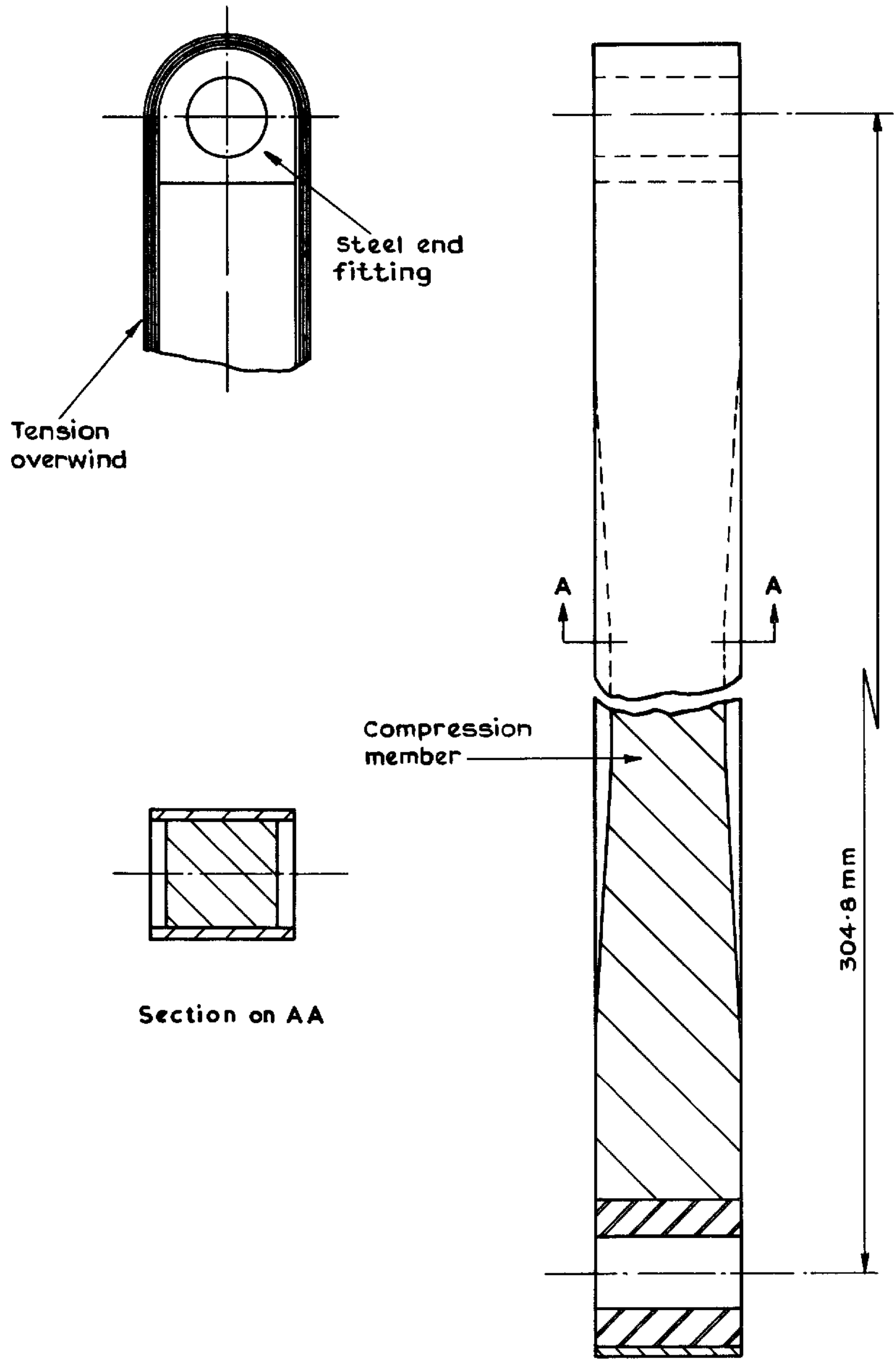

Fig.4 GRP strut

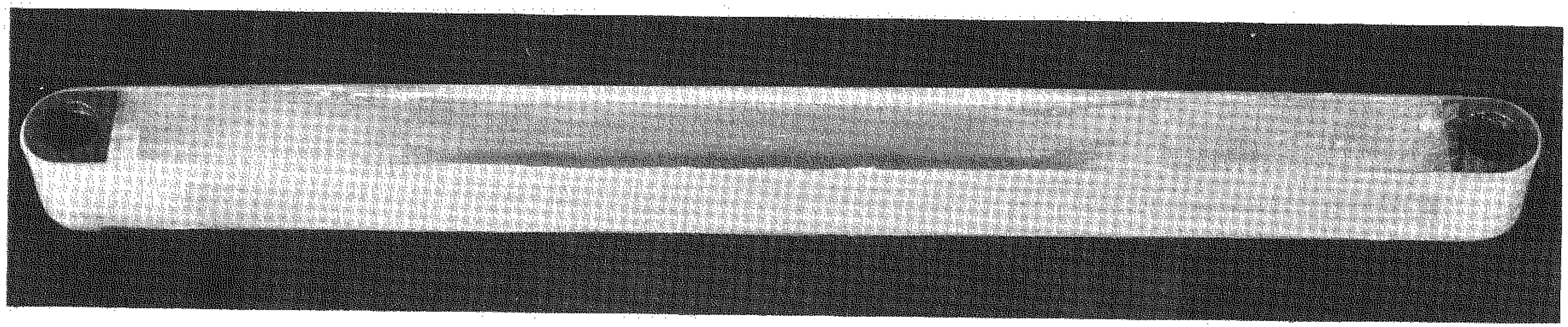

Fig.5 GRP strut

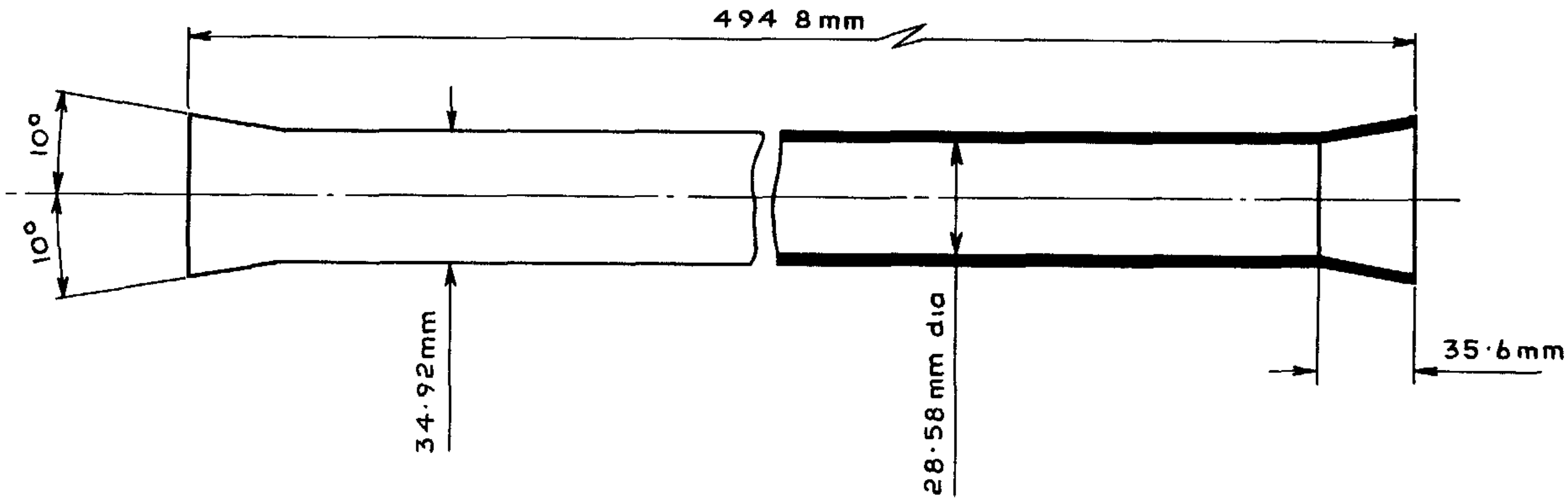

Fig.6 CFRP tube for struts models one and two

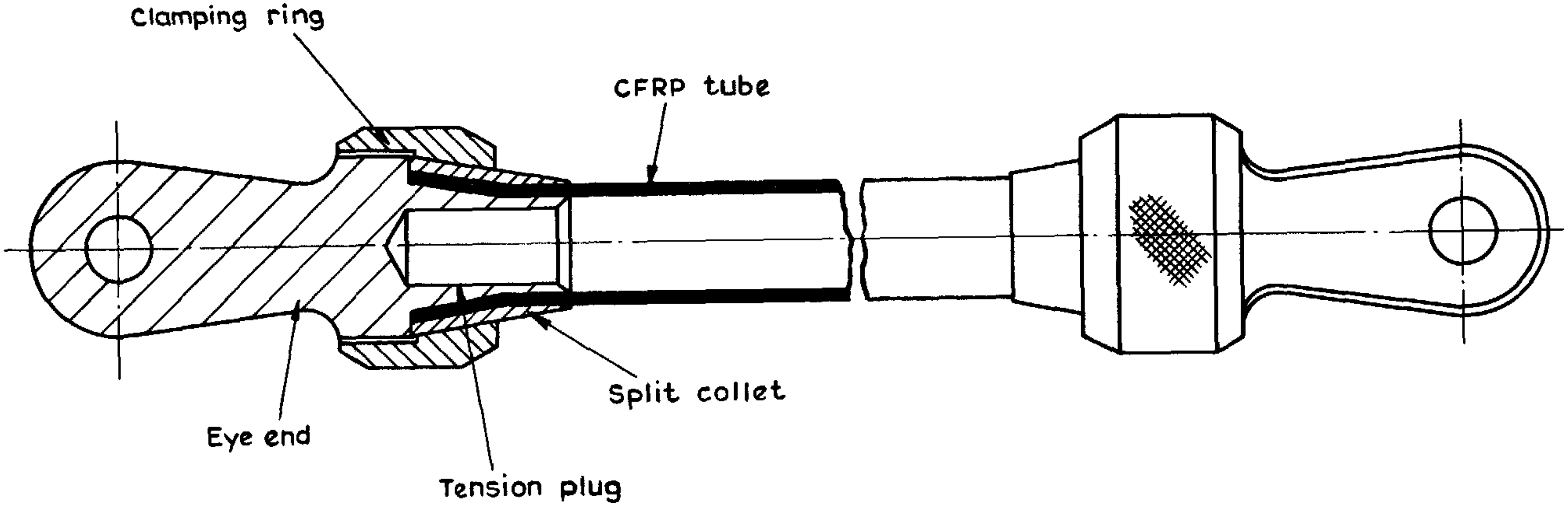

Fig.7 End fitting assembly for CFRP strut model one

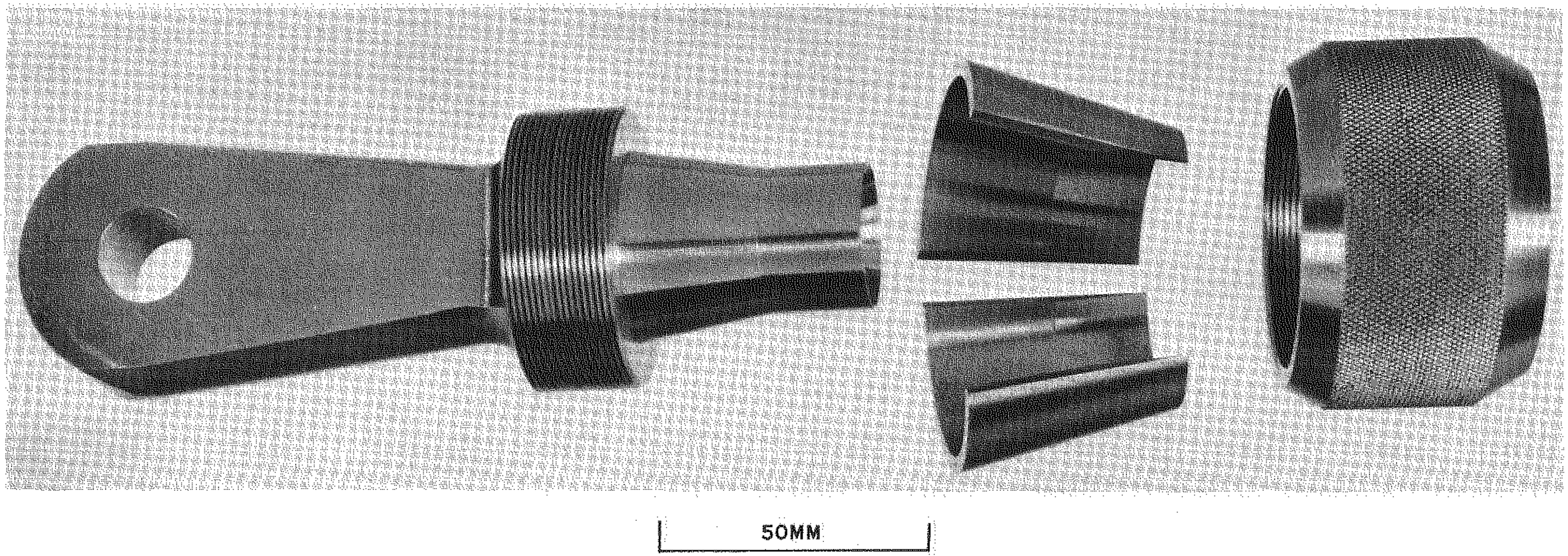

Fig.8 End fitting components of CFRP strut model 1

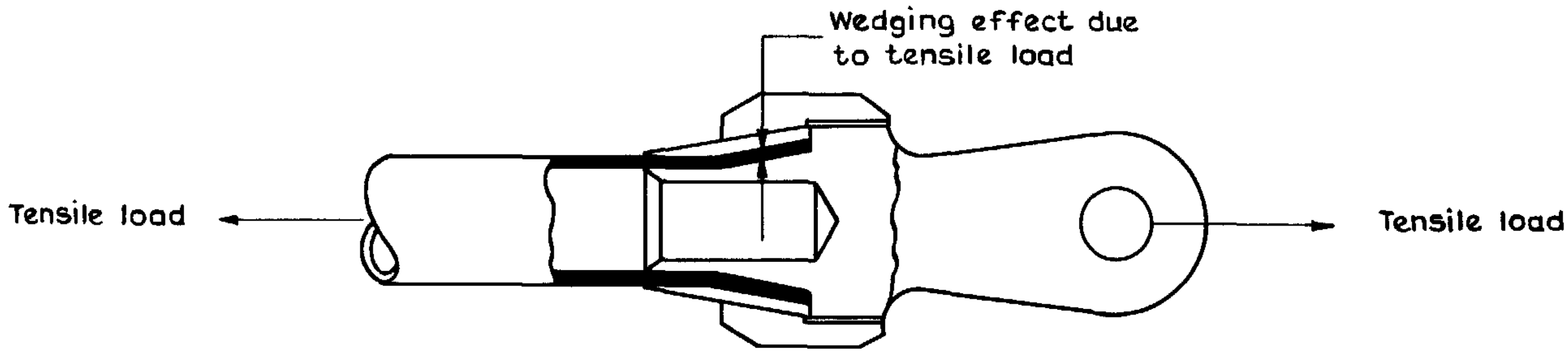

Fig.9 End fitting loaded in tension

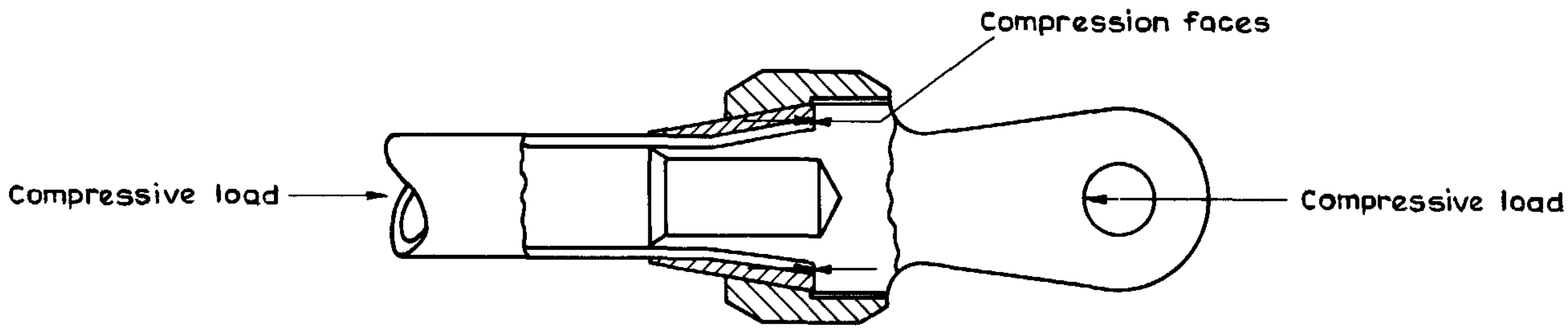

Fig.10 End fitting loaded in compression

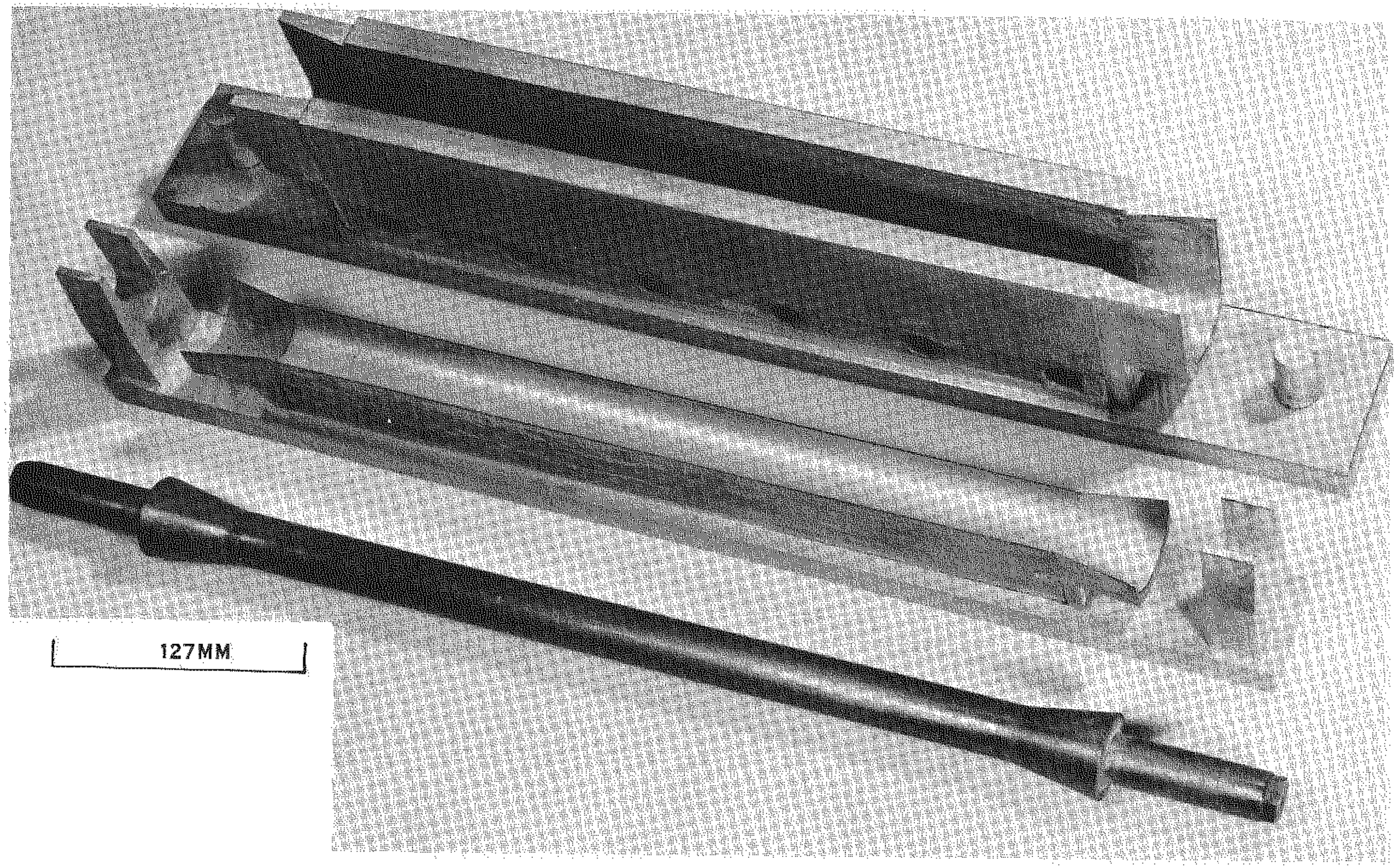

Fig.11 Tube mould

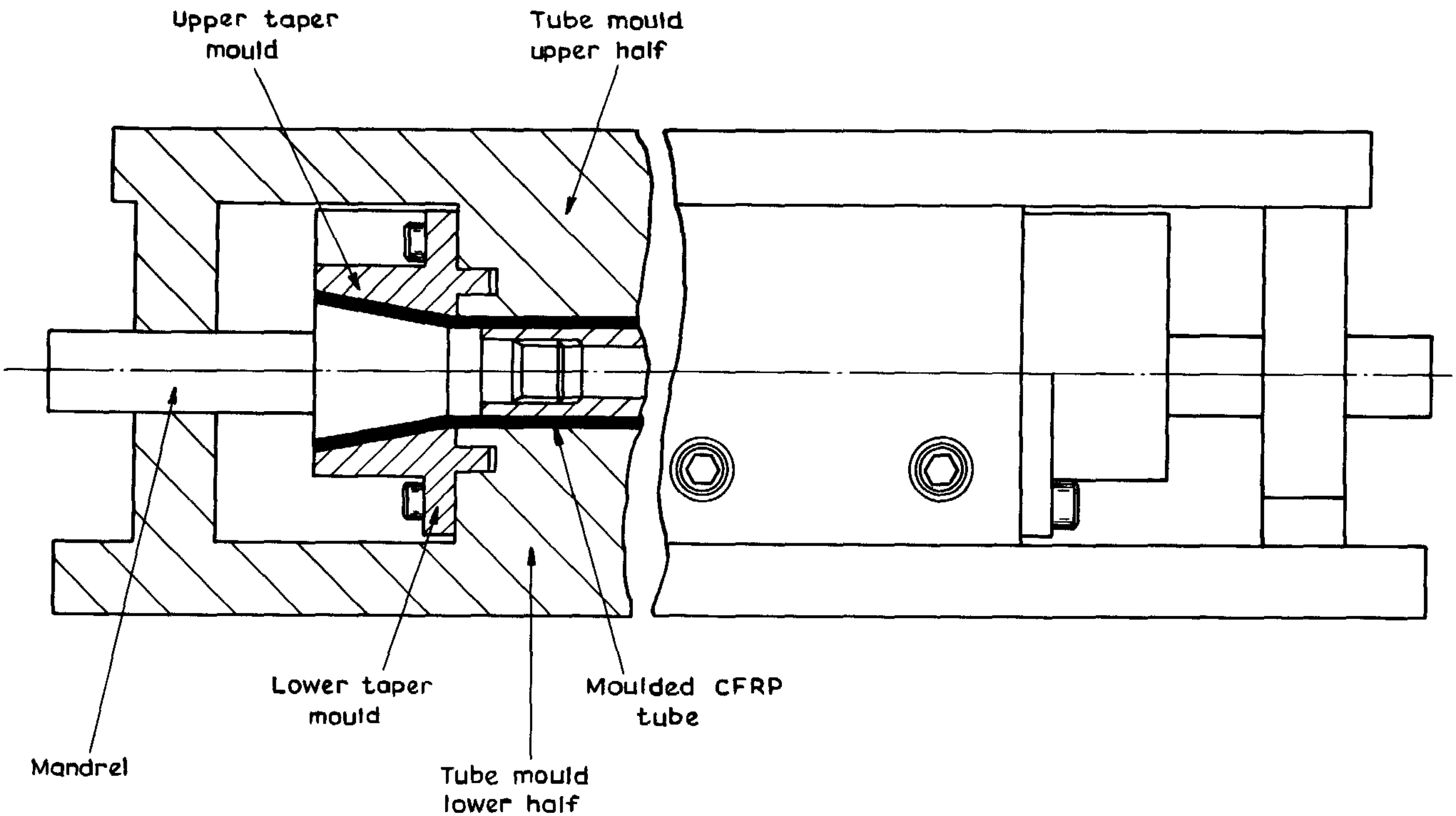

Fig.12 Tube mould assembly

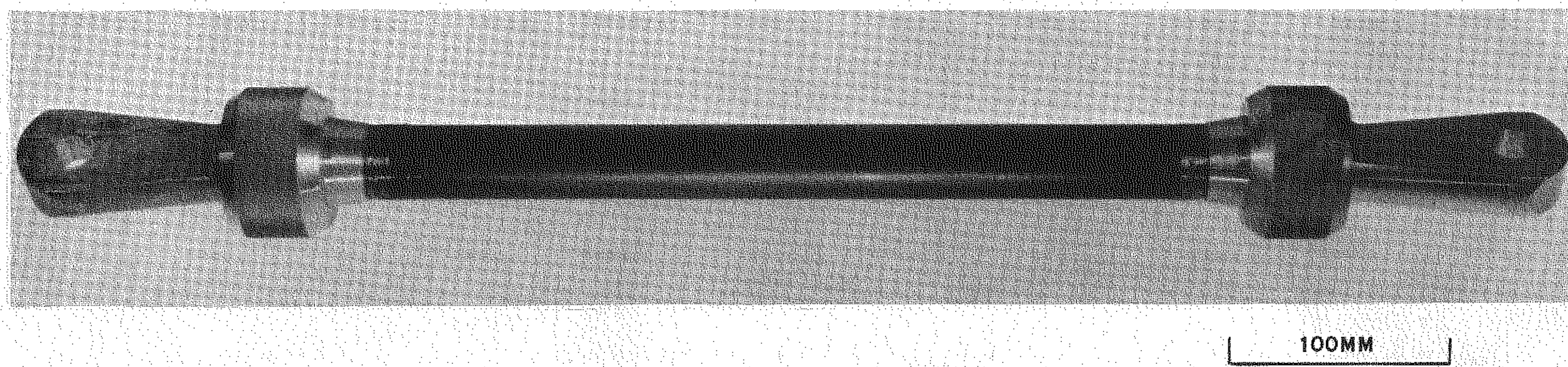

Fig.13 Assembly of CFRP strut models 1 and 2

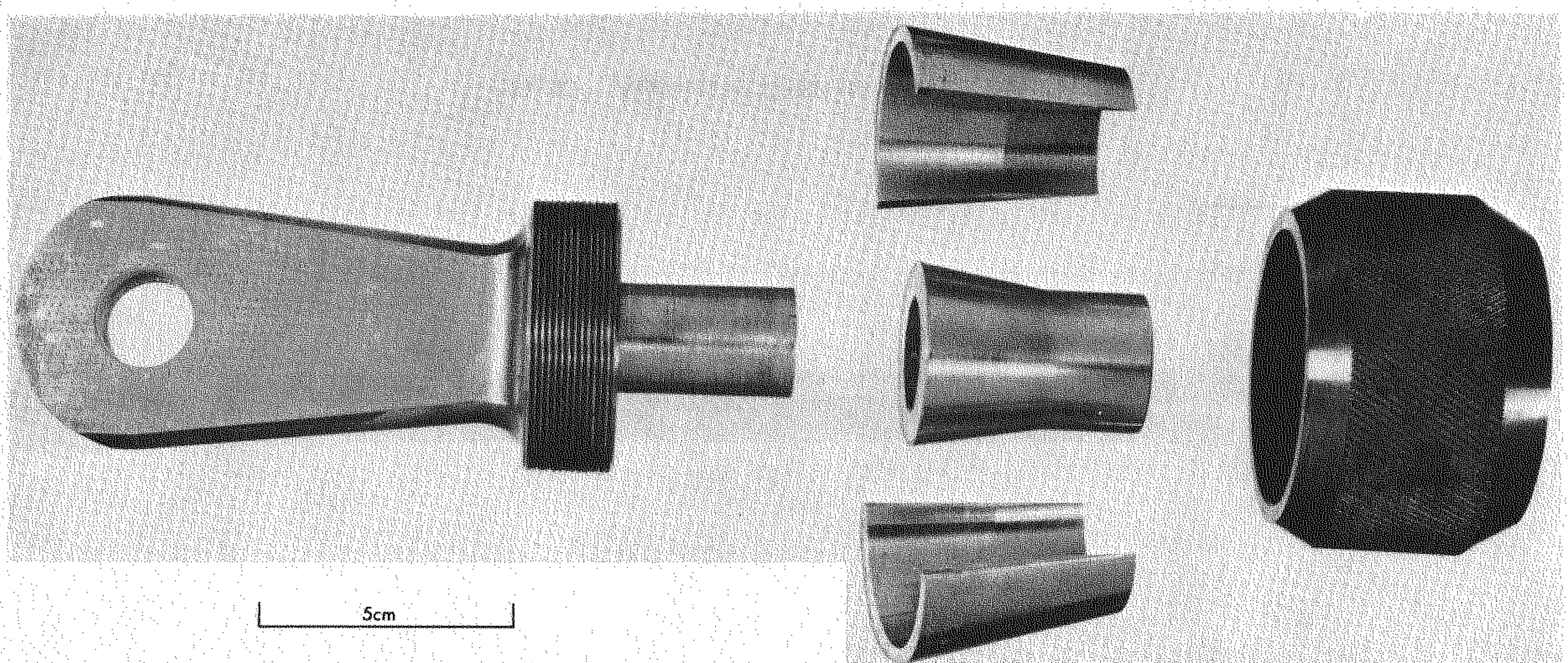

Fig.14 End fitting components for CFRP strut model 2

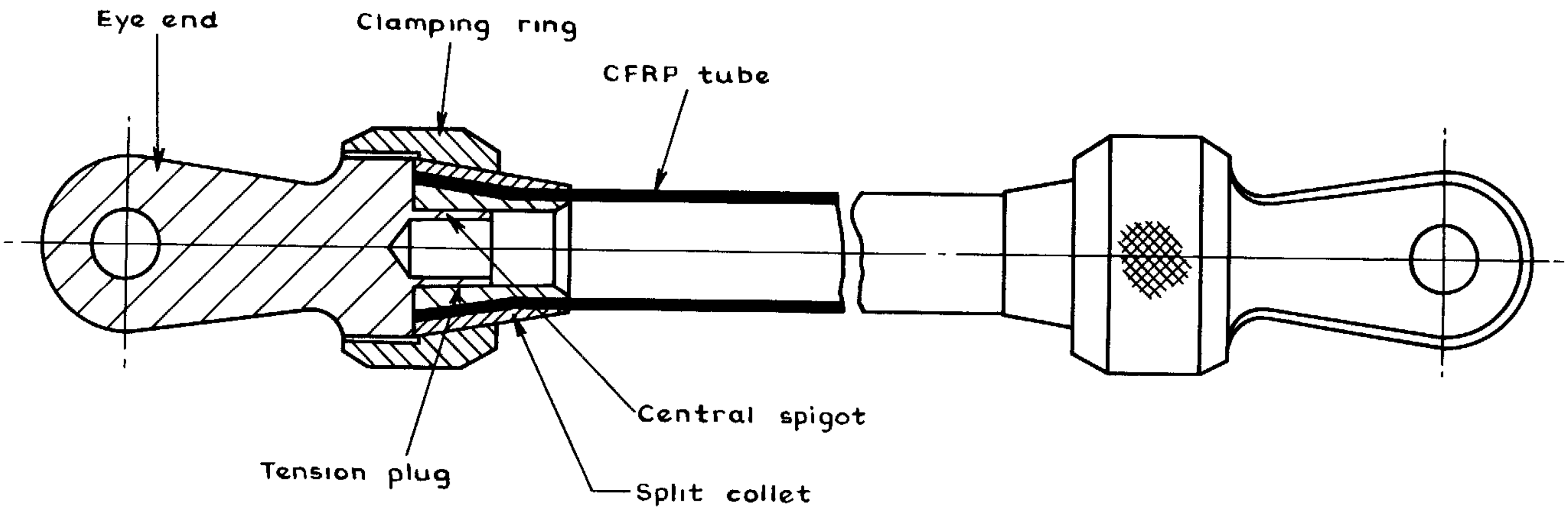

Fig. 15 Strut assembly of CFRP strut model two

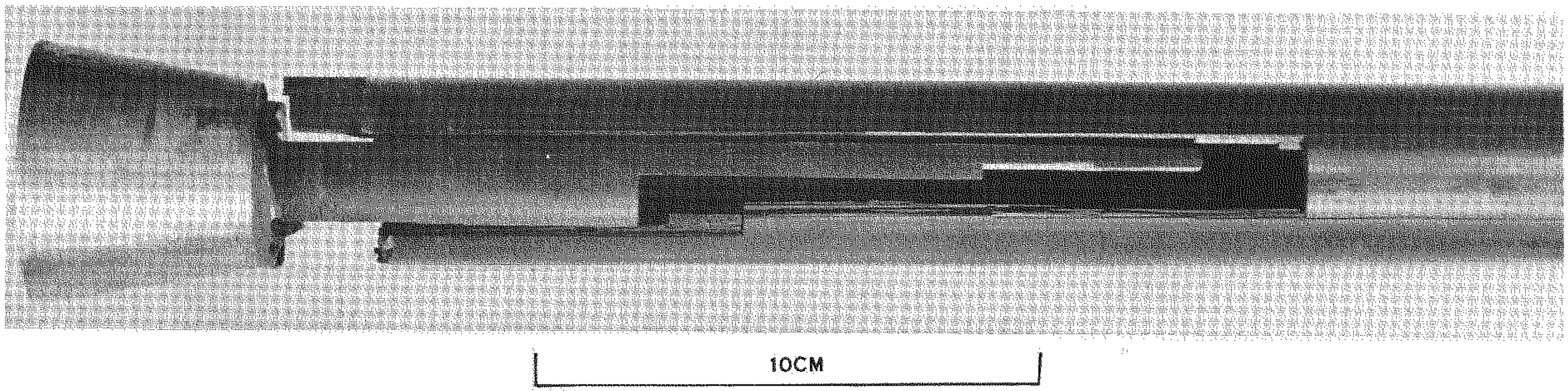

Fig.16 Tension failure CFRP strut model 2/II

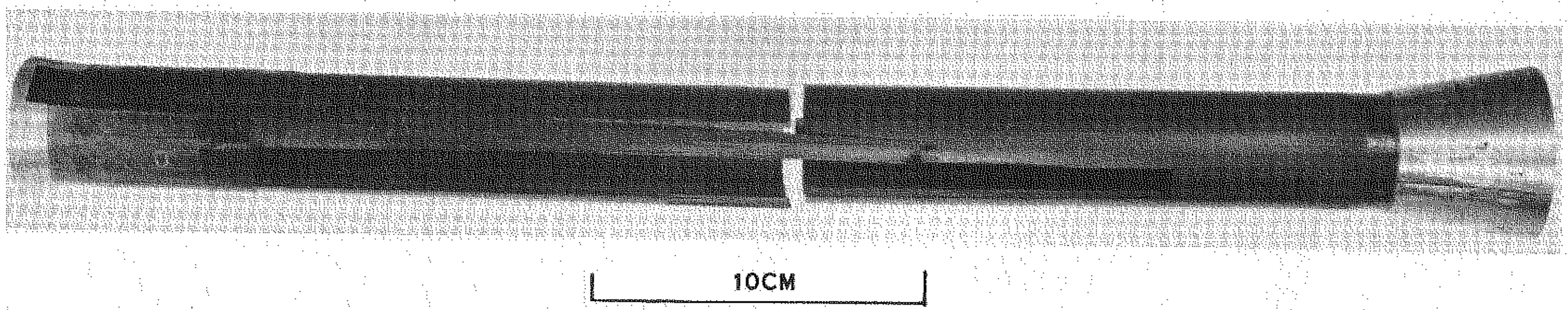

Fig.17 Tension failure CFRP strut model 2/III

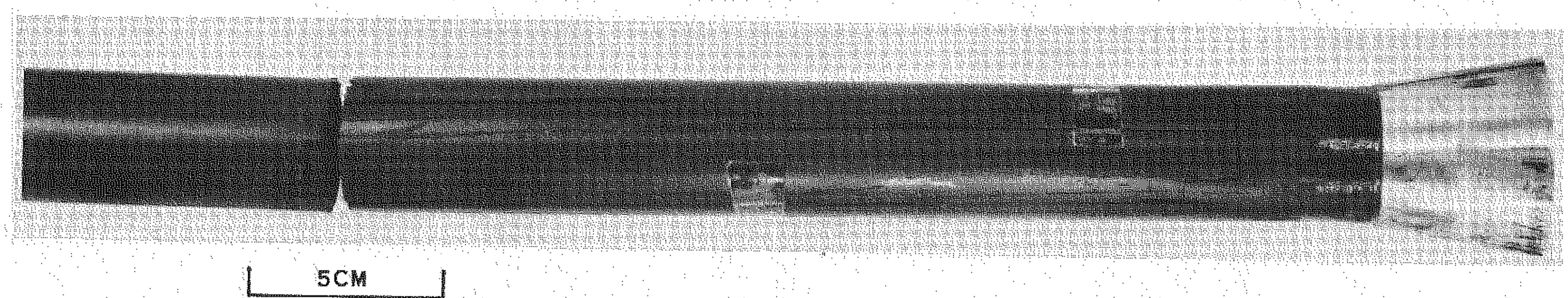

Fig.18 Tension failure CFRP strut model 2/IV

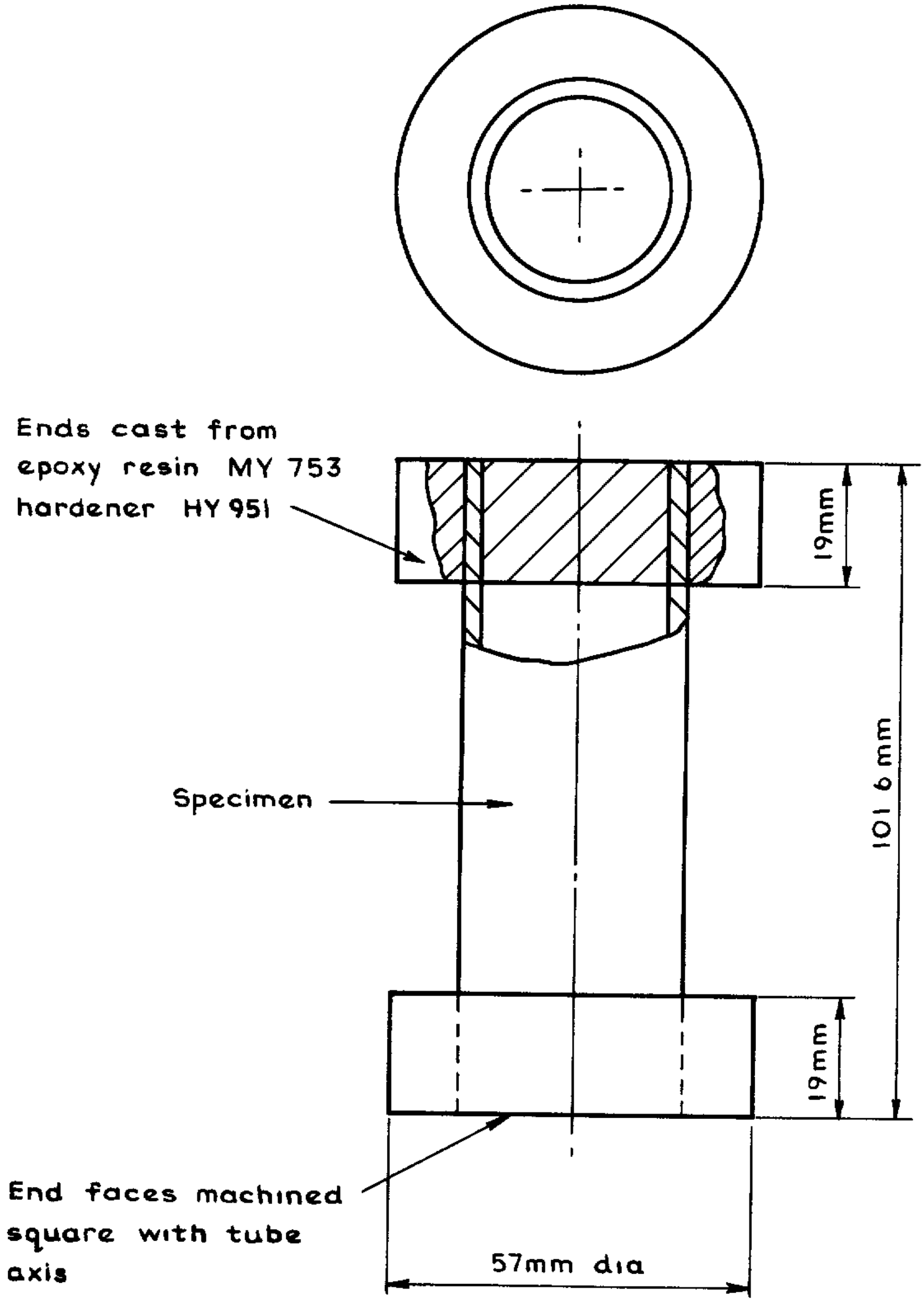

Fig. 19 Compression test specimen

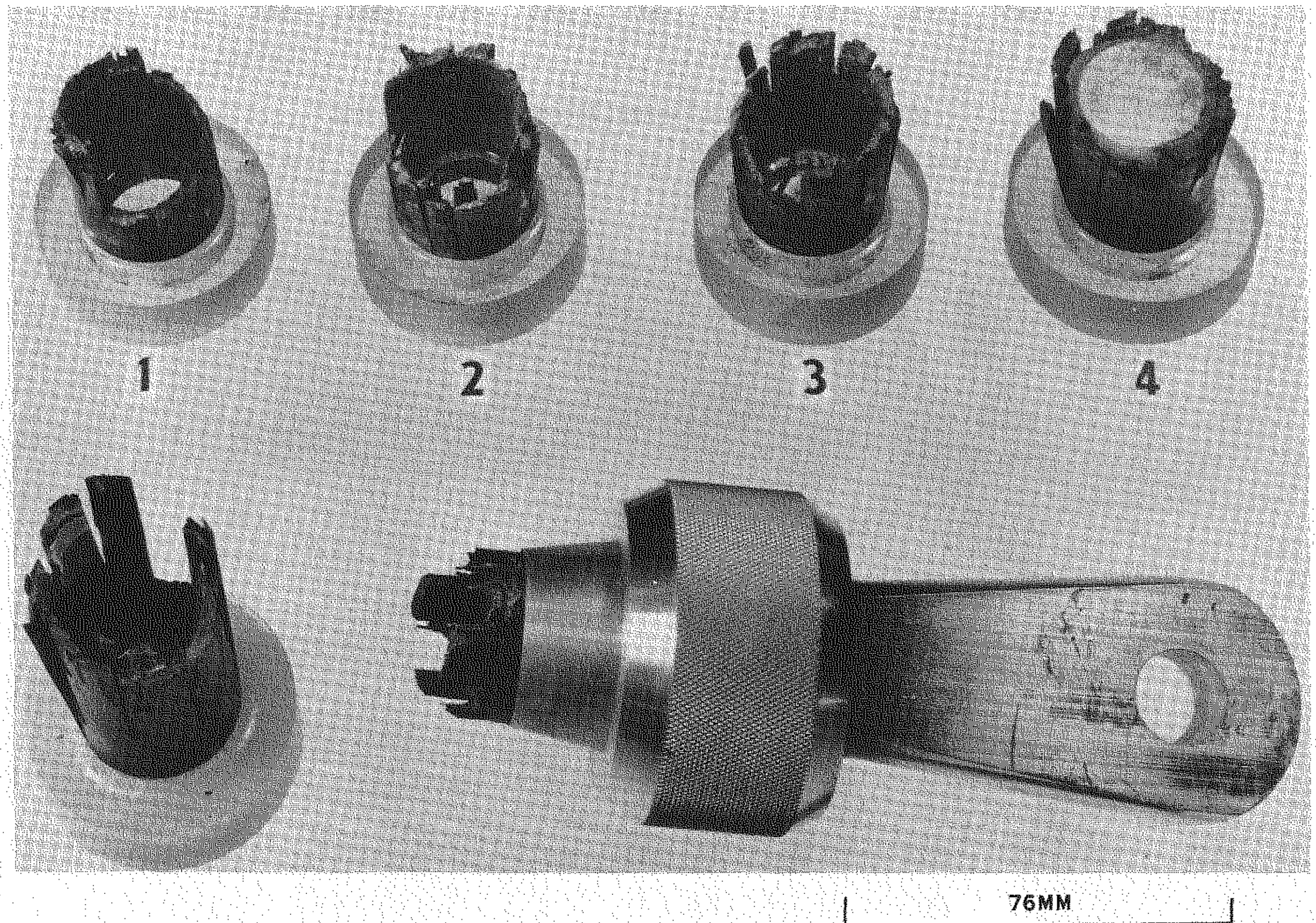

Fig.20 Failed compression specimens

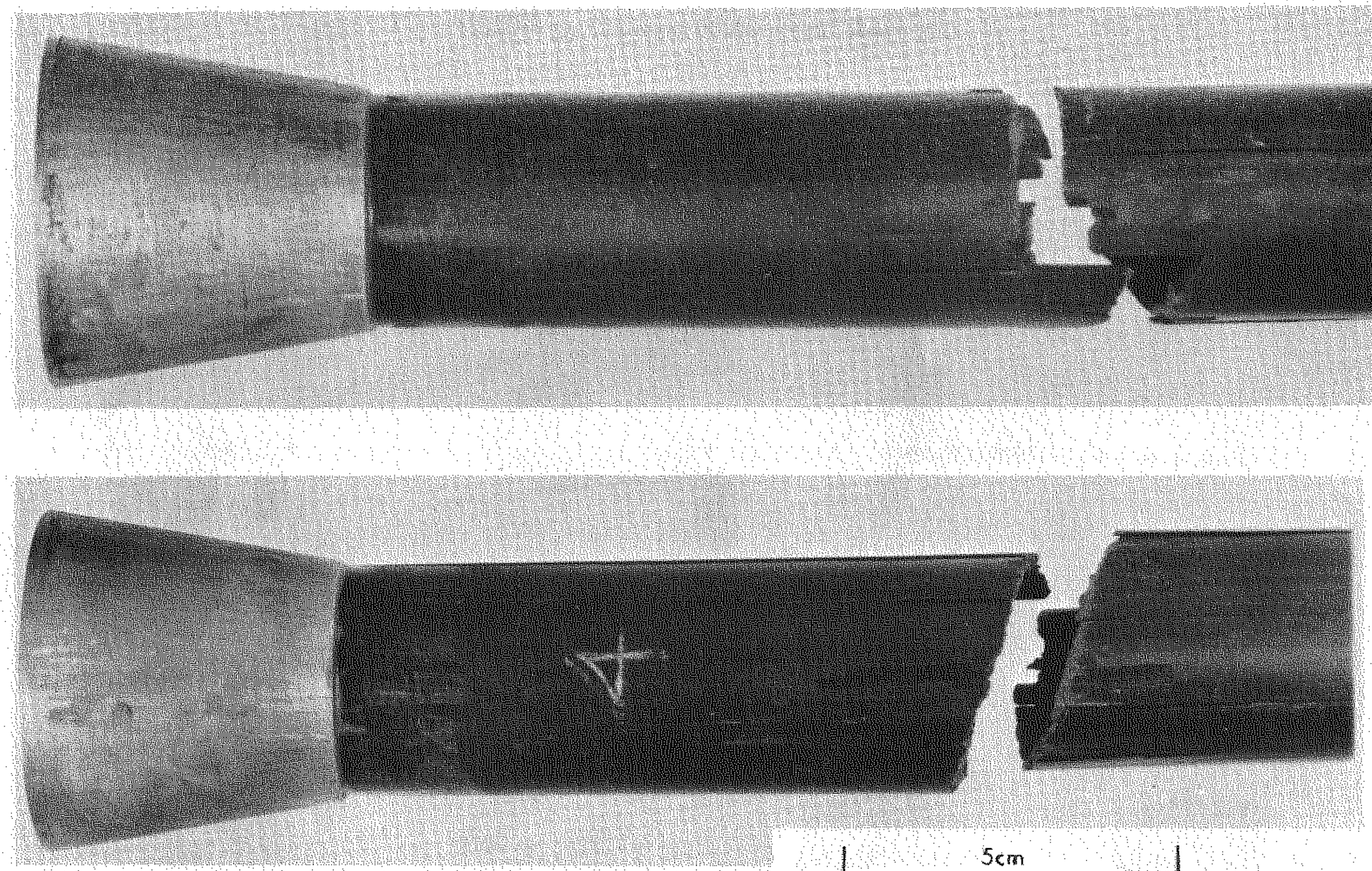

Fig.21 Compression failure CFRP strut model 2

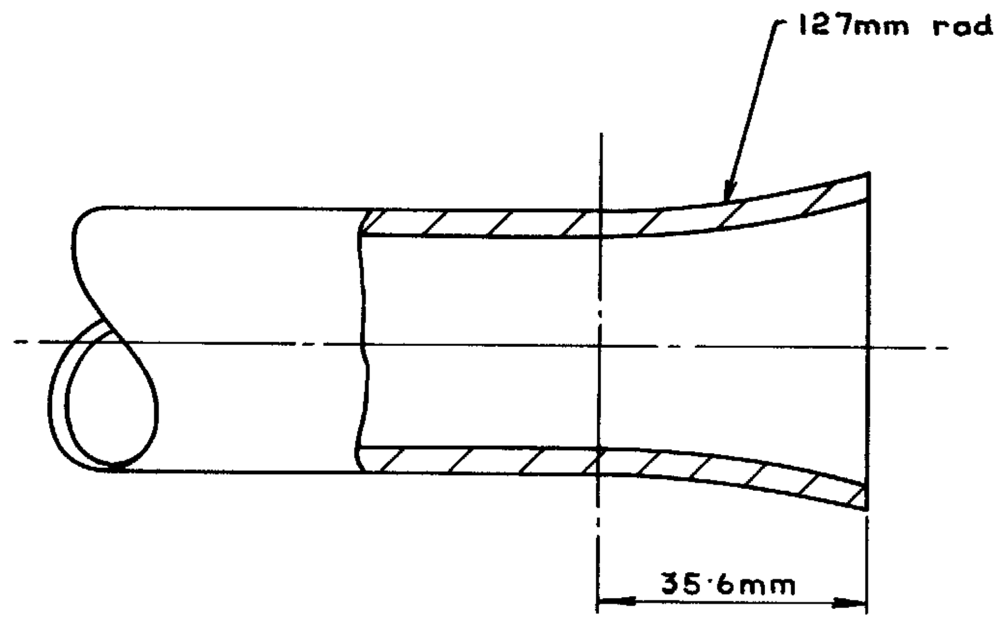

Fig. 22 Radiused tube end CFRP strut models three and four

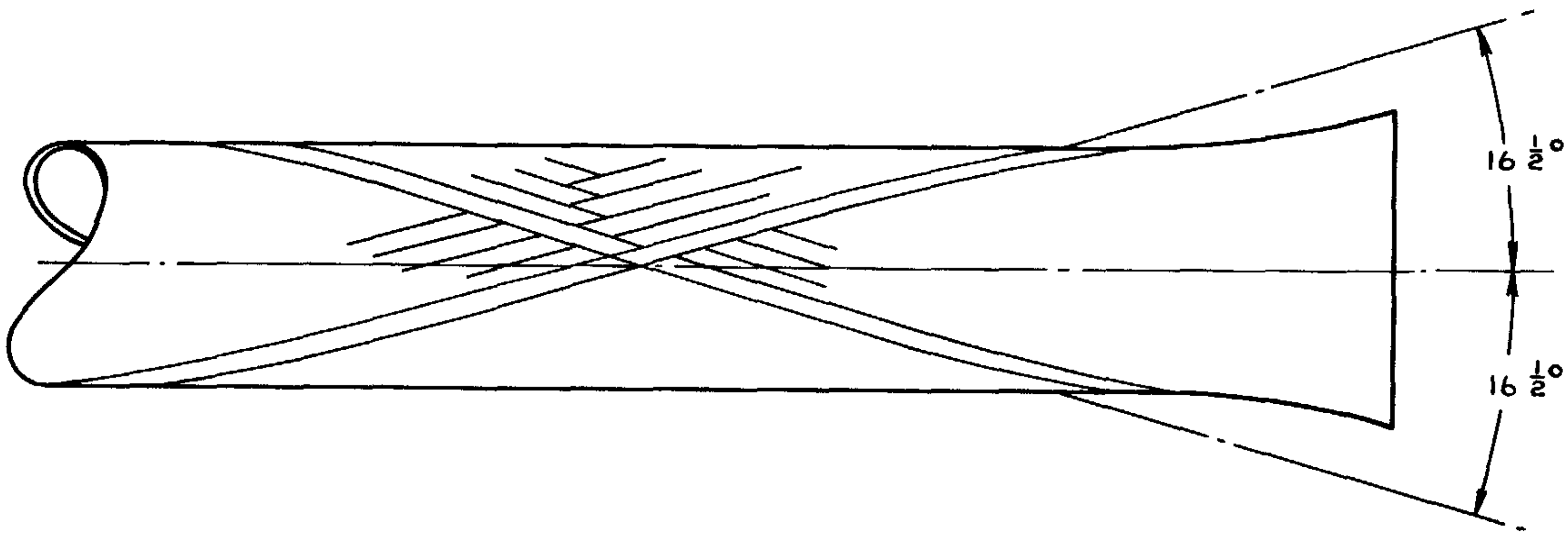

Fig. 23 Winding reinforcement geometry

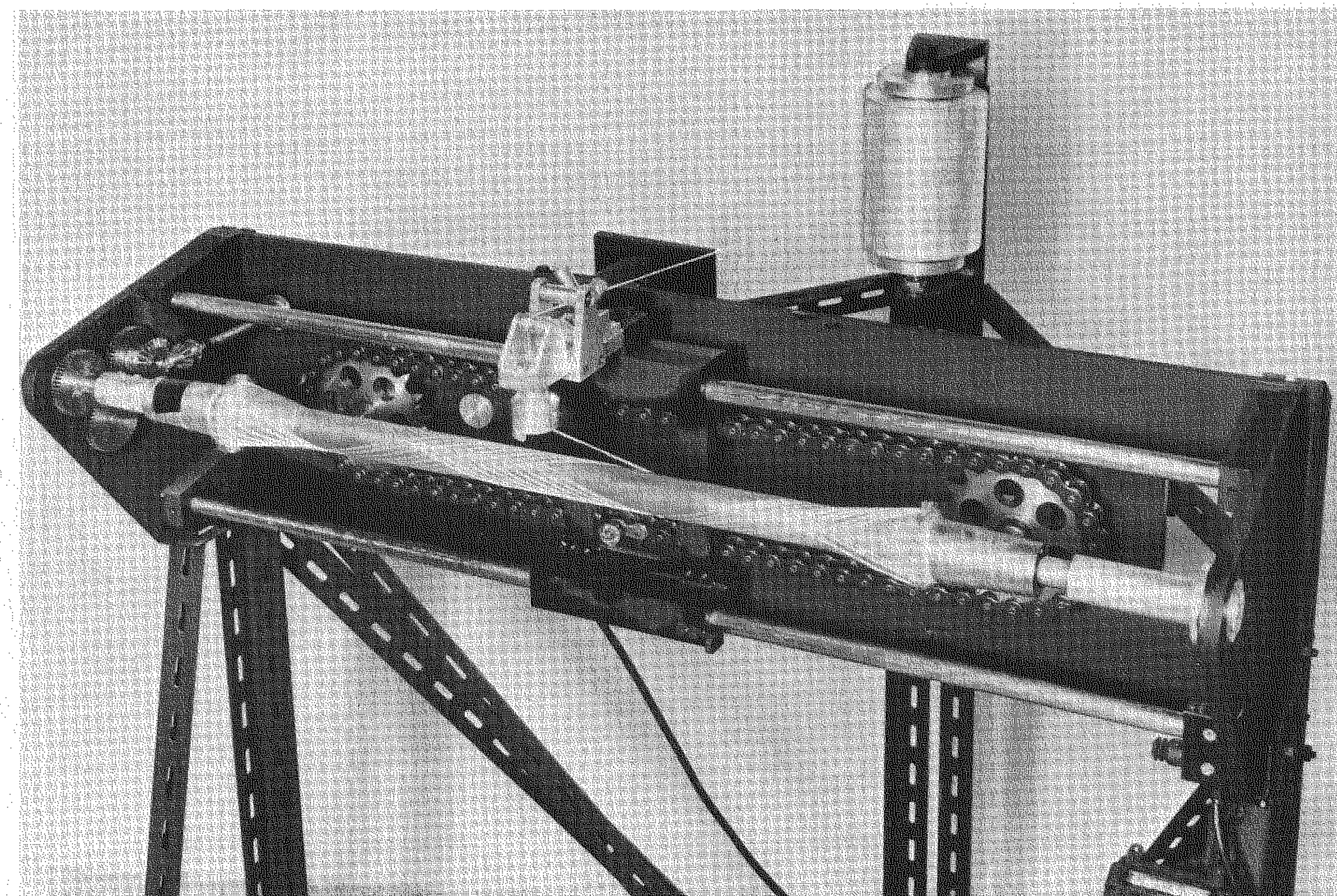

Fig.24 Filament winding machine

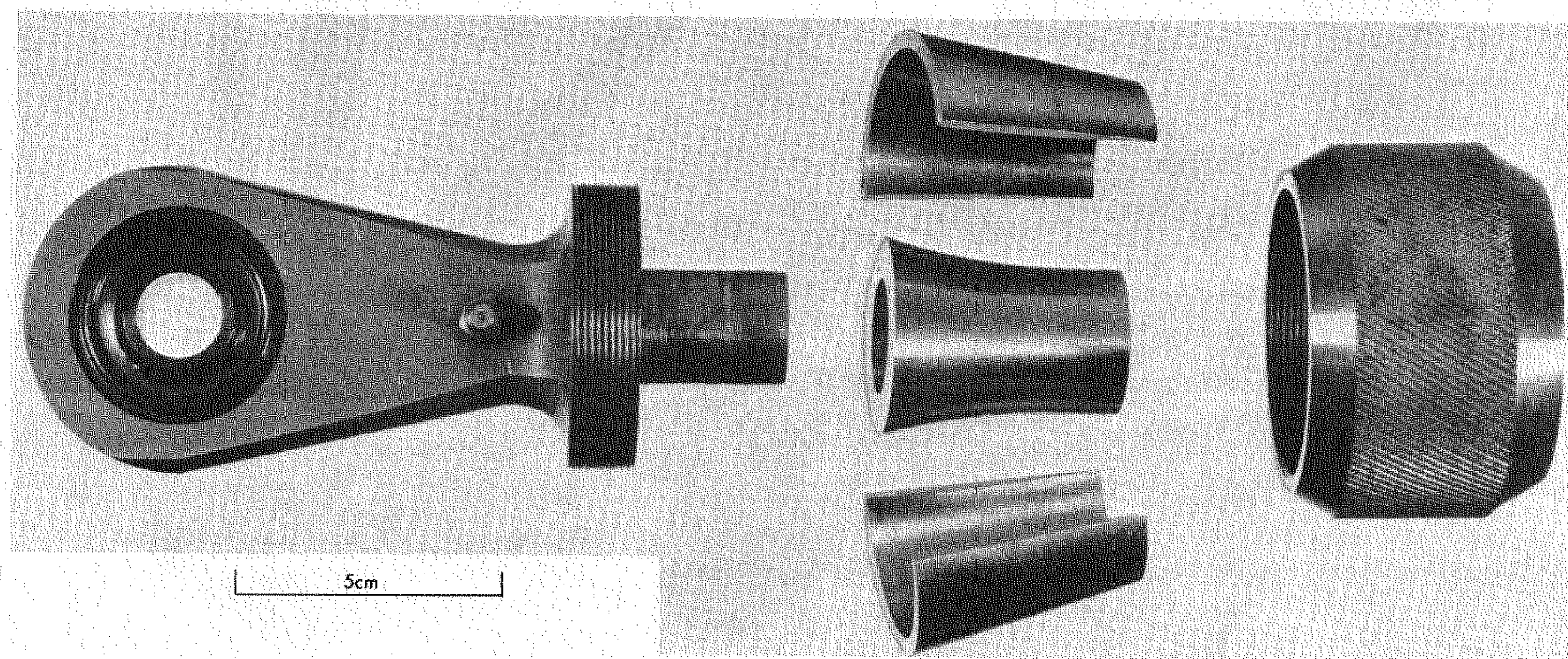

Fig.25 End fitting components for CFRP strut model 3

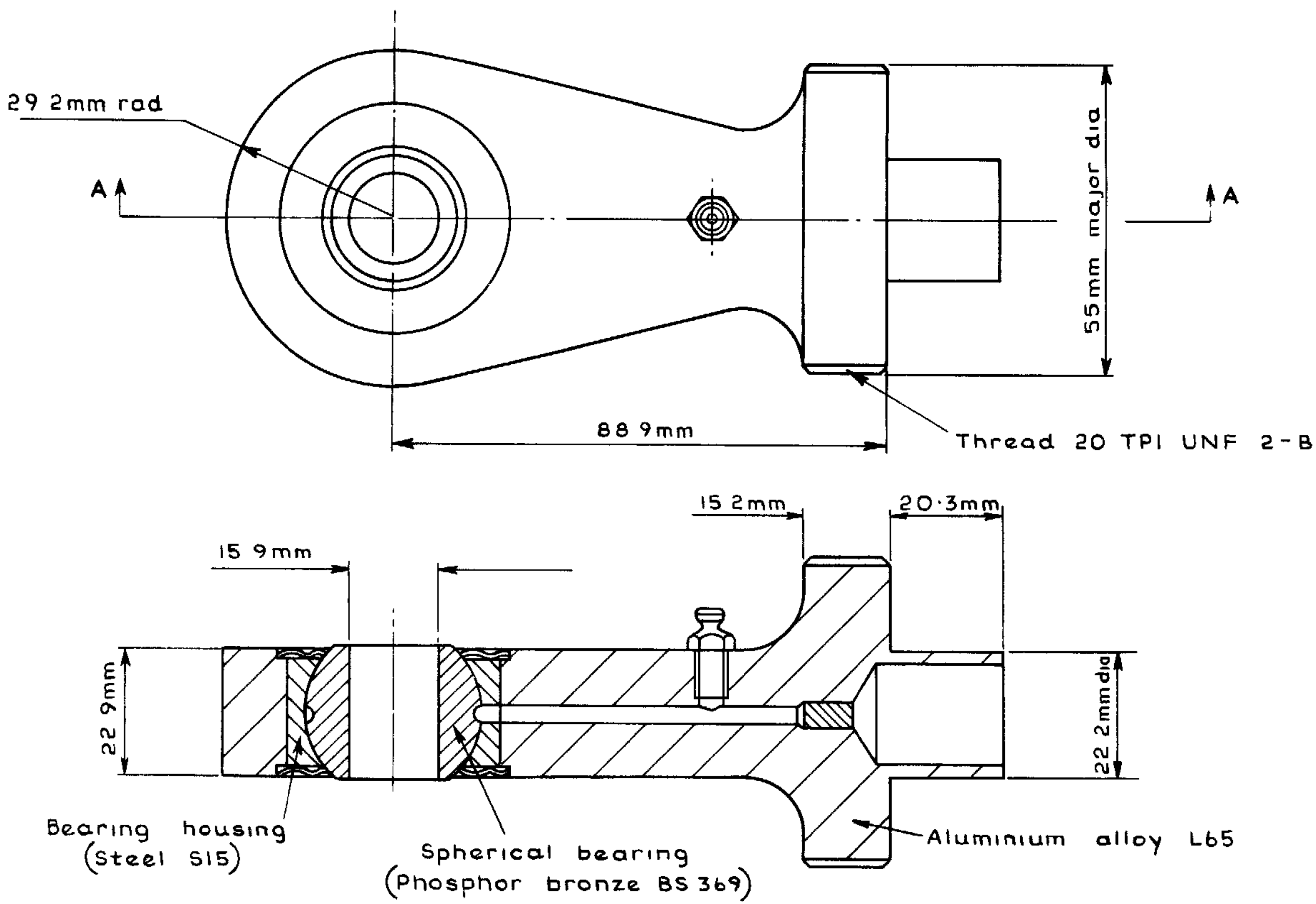

Fig. 26 Eye end

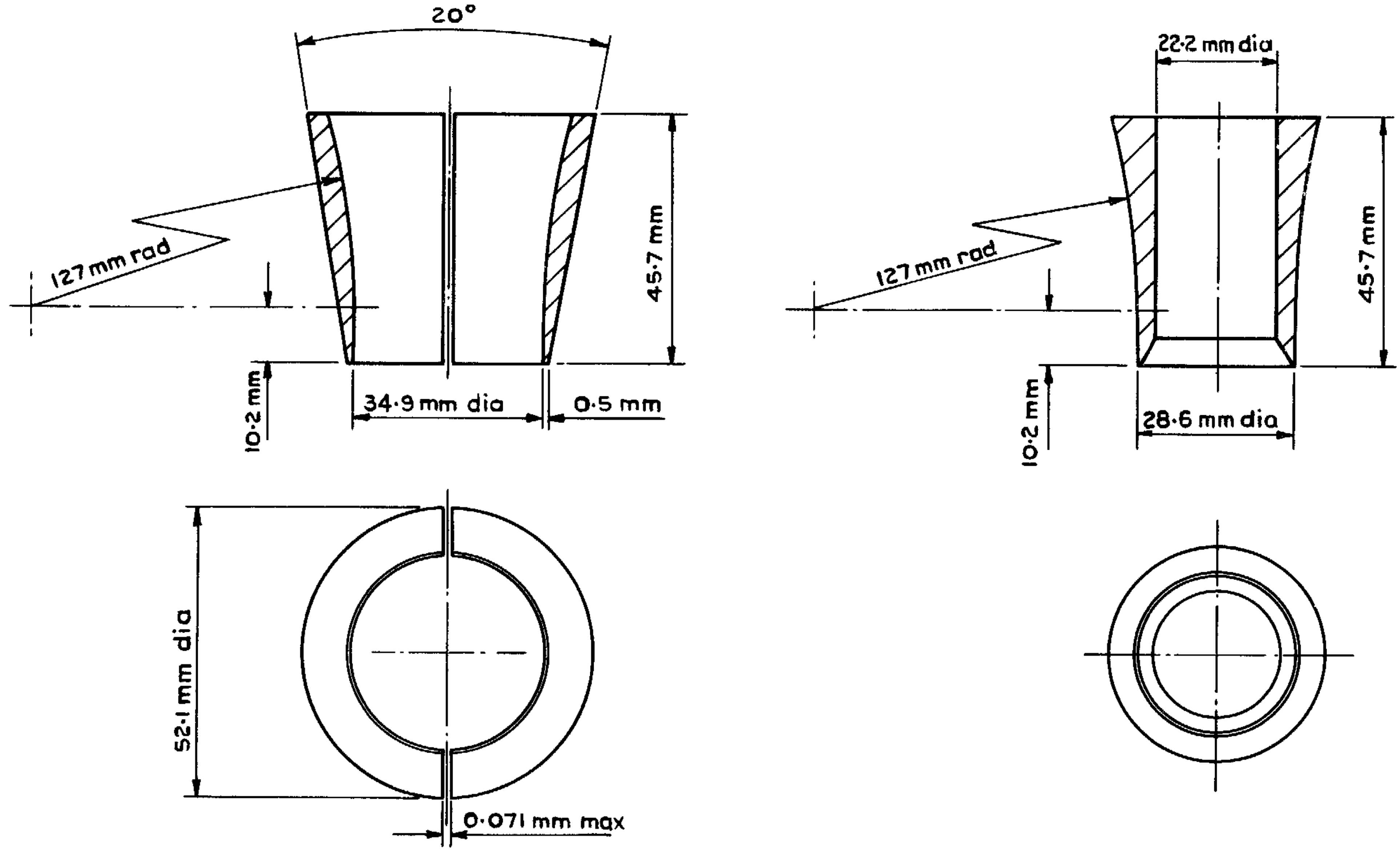

Fig. 27 Split collet and tension plug

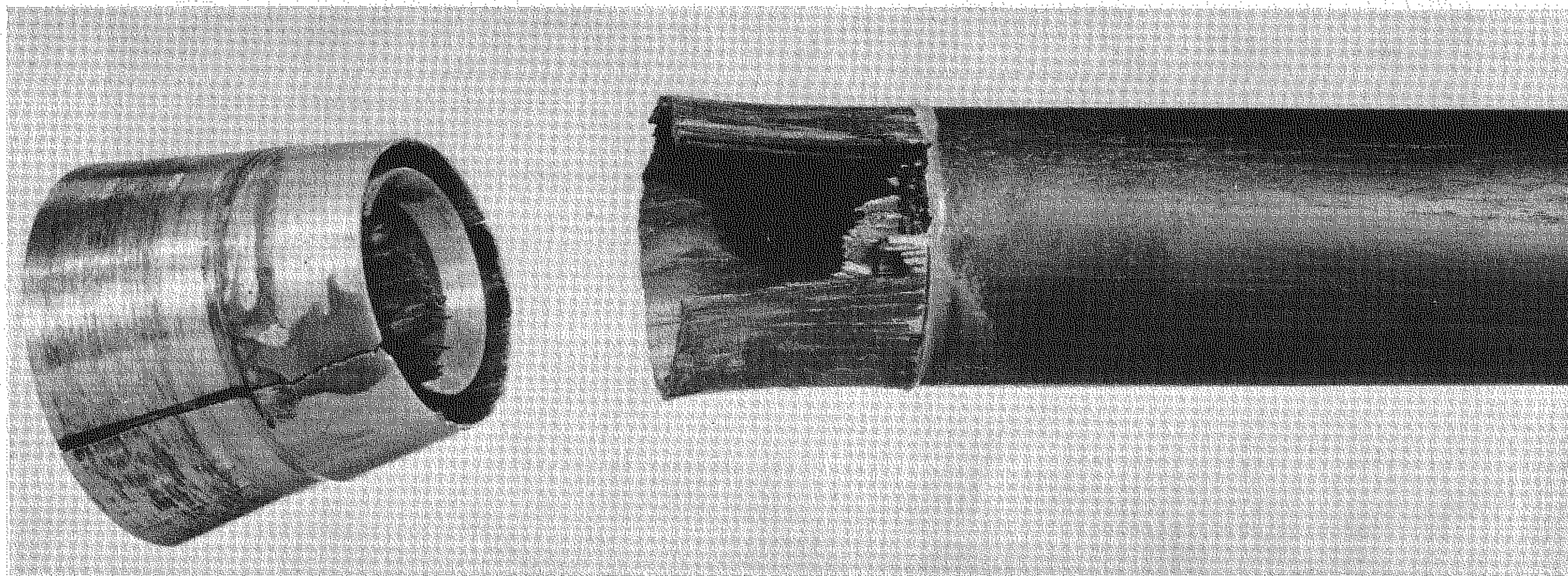

Fig.28 Tension failure CFRP strut model 3

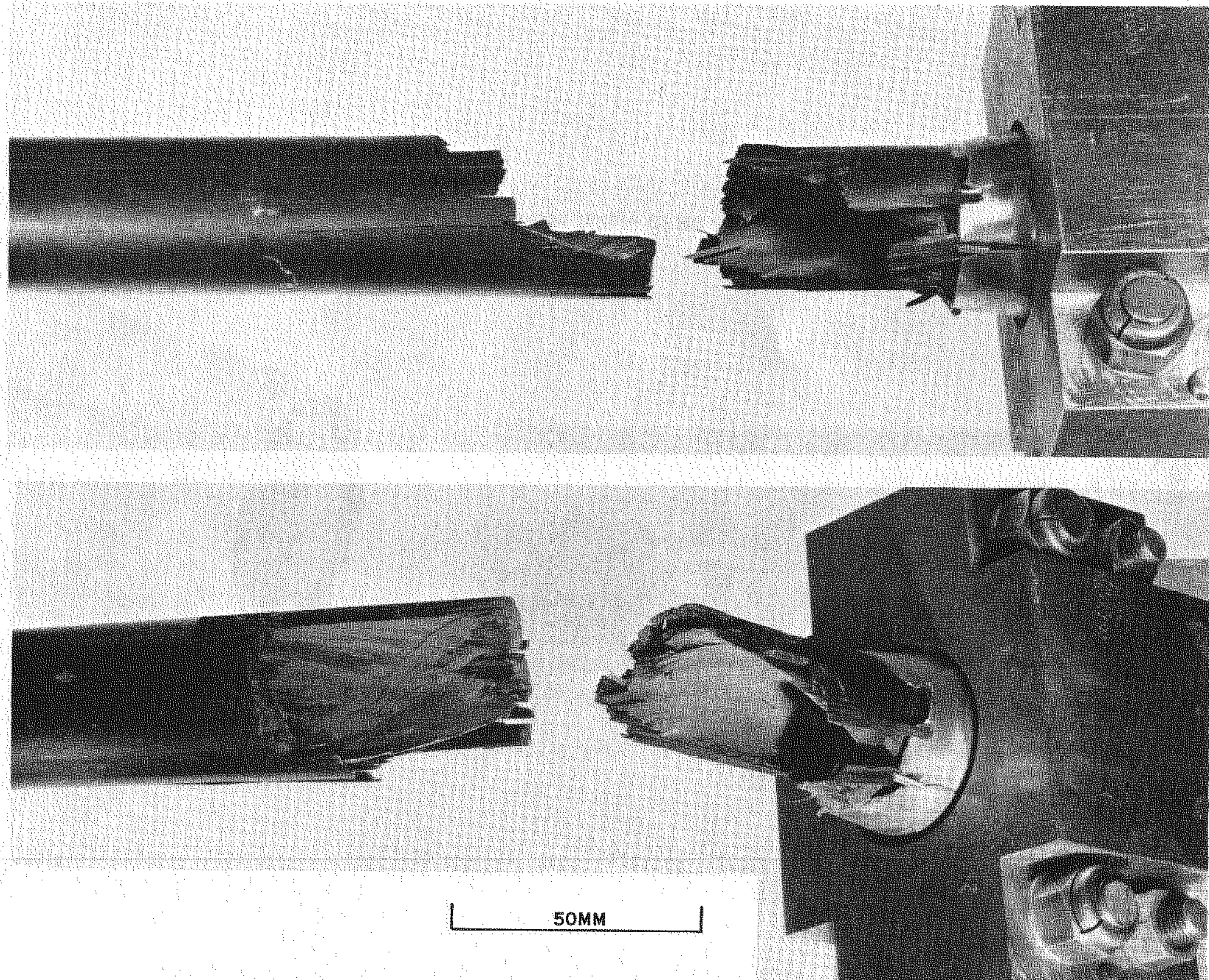

Fig.29 Compression failure CFRP strut model 3

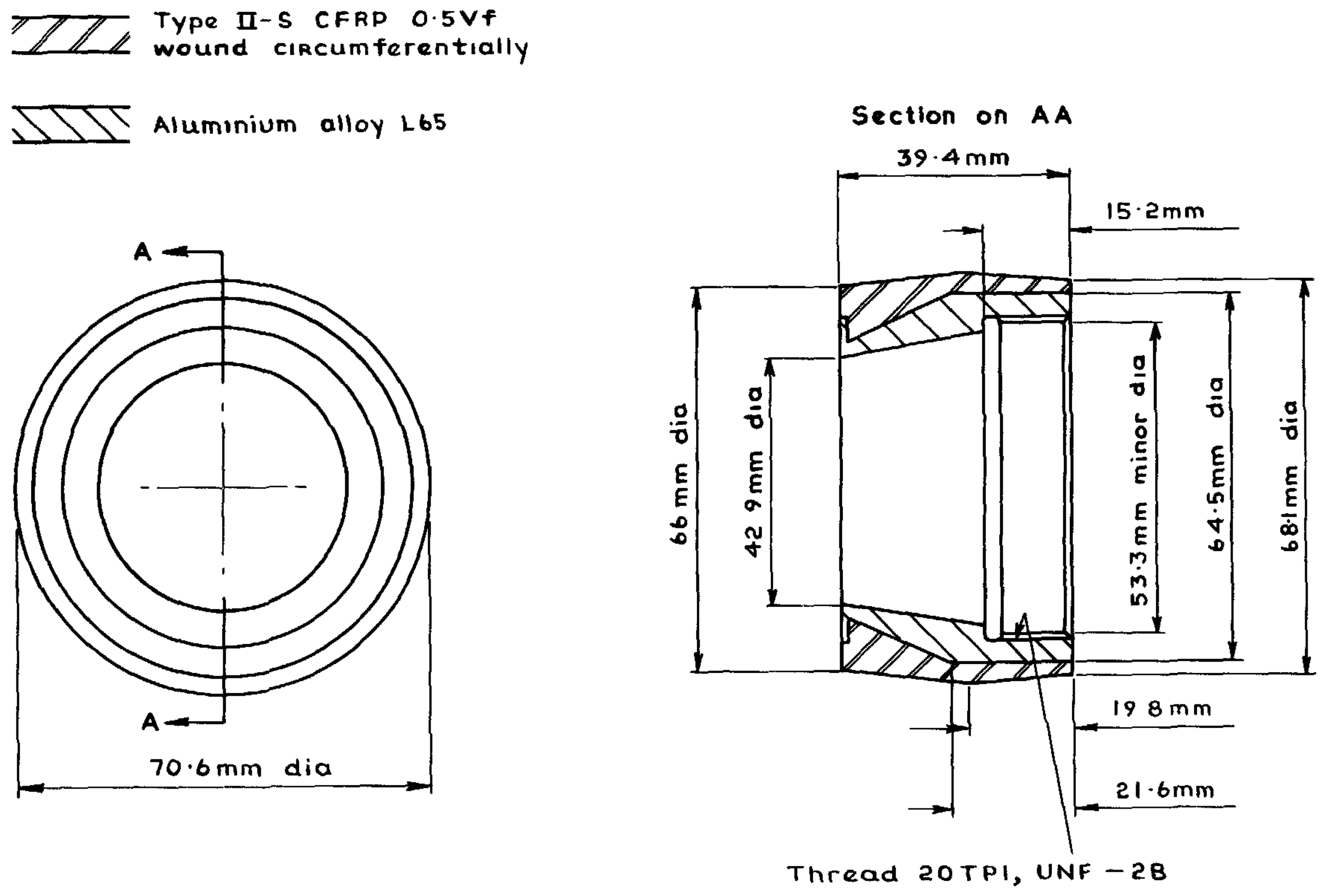

Fig. 30 Clamping ring

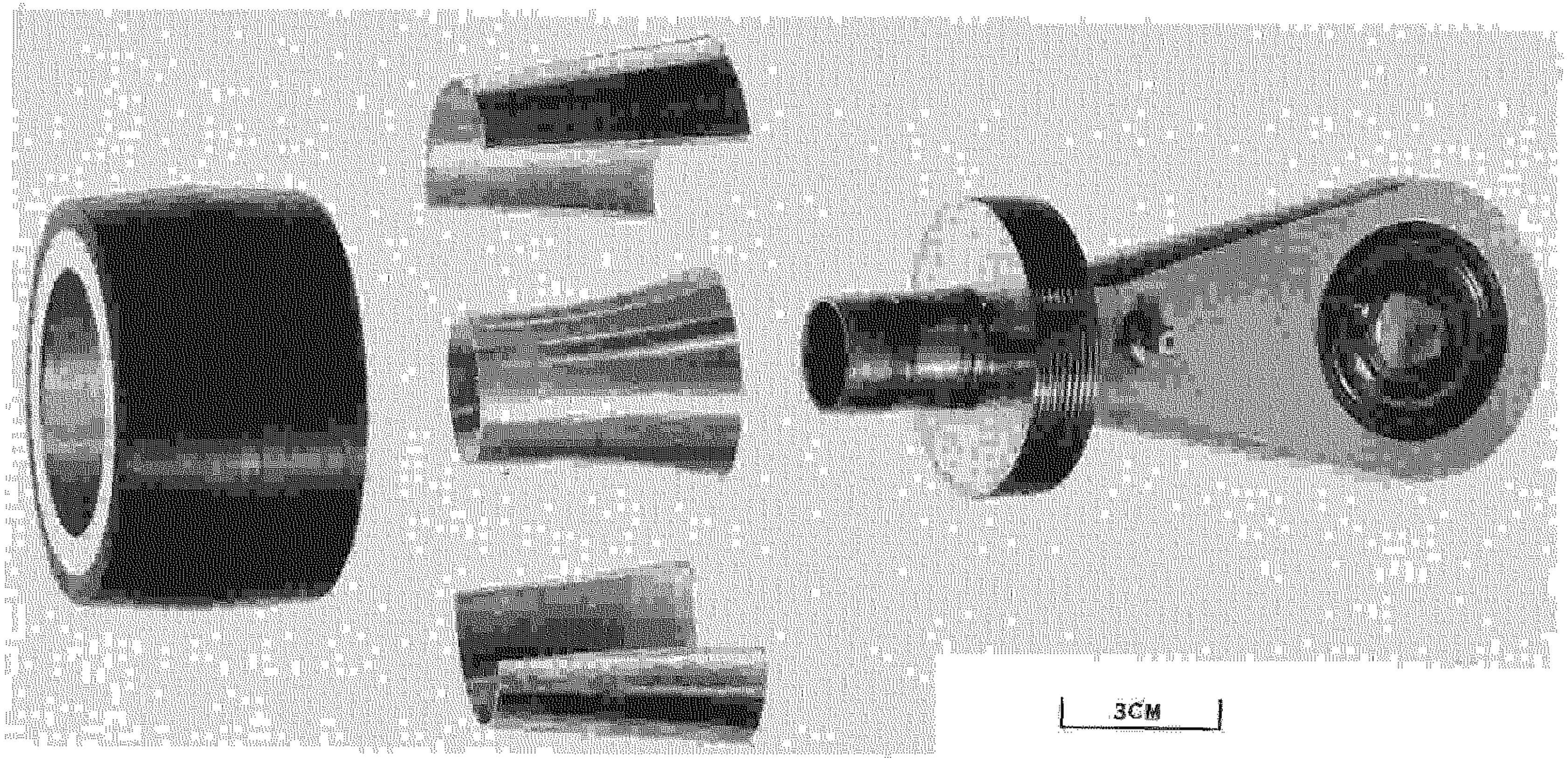

Fig.31 Finalised end fitting components

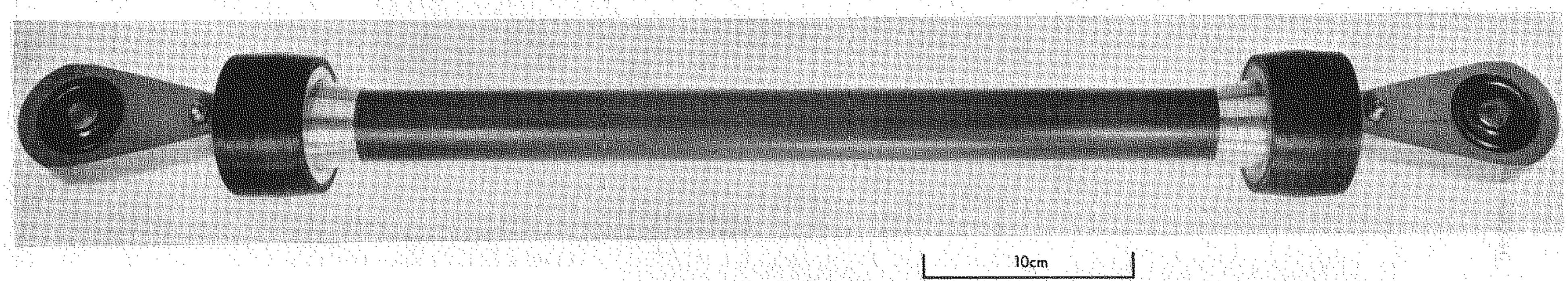

Fig.32 Finalised strut assembly

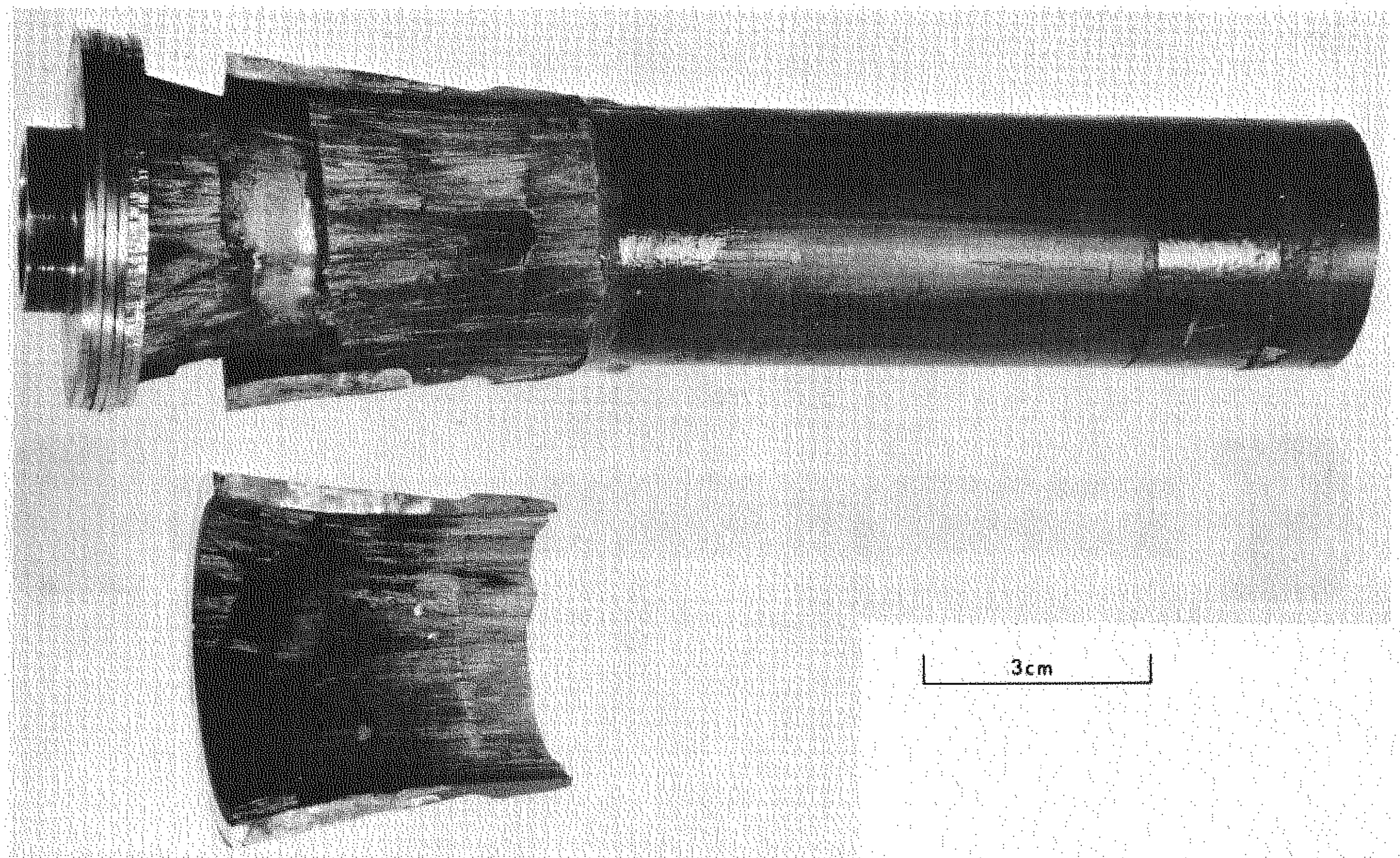

Fig.33 Tension failure CFRP strut model 4

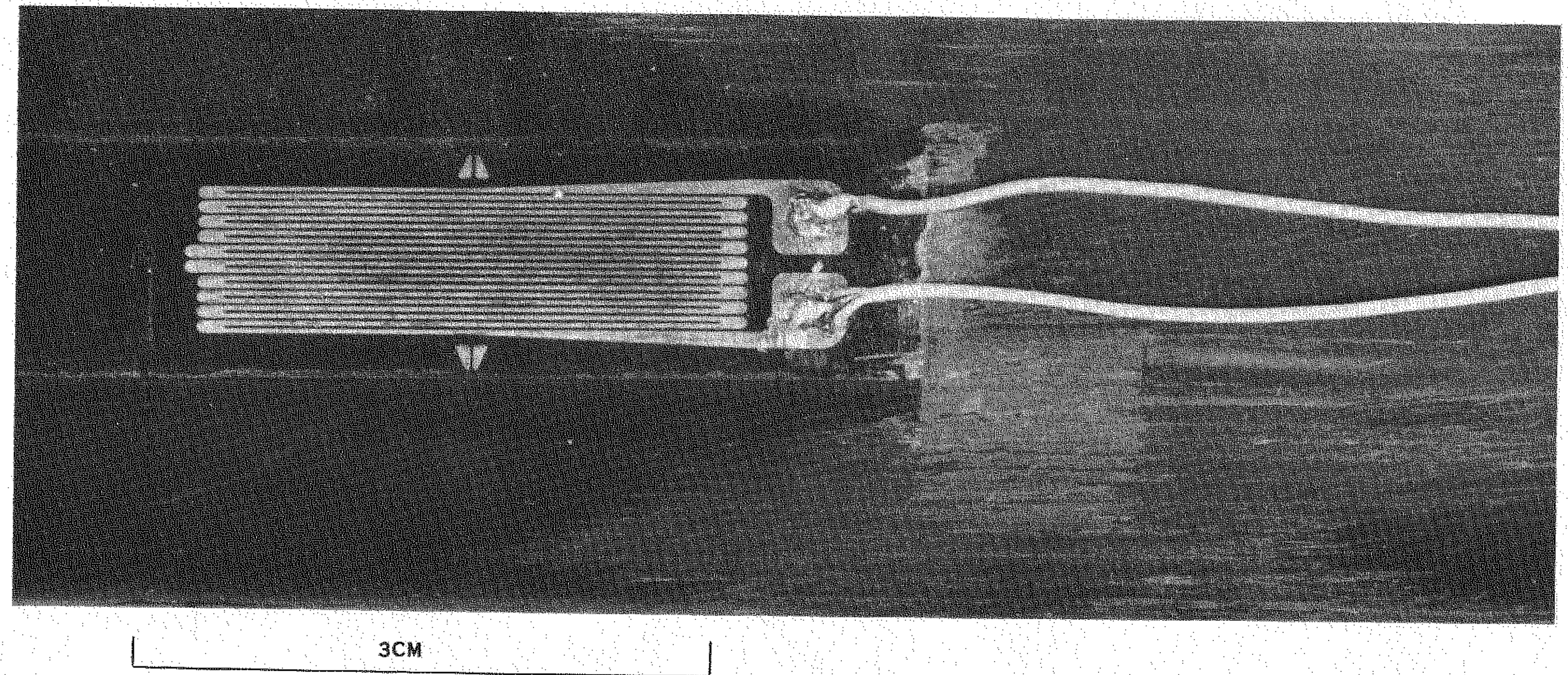

Fig.34 Strain gauging for CFRP tube moduli

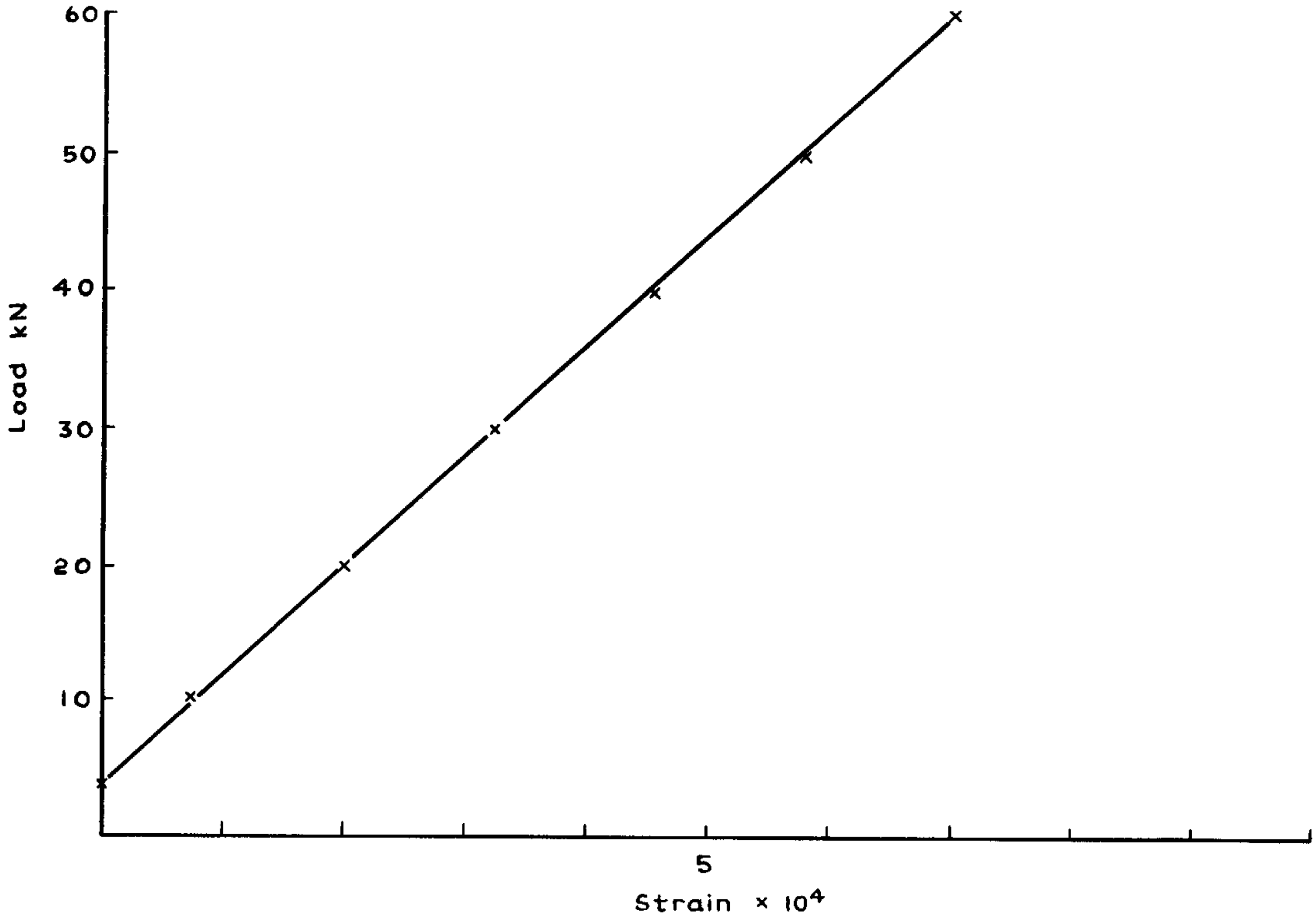

Fig. 35 Variation of strain with load for CFRP tube loaded in tension

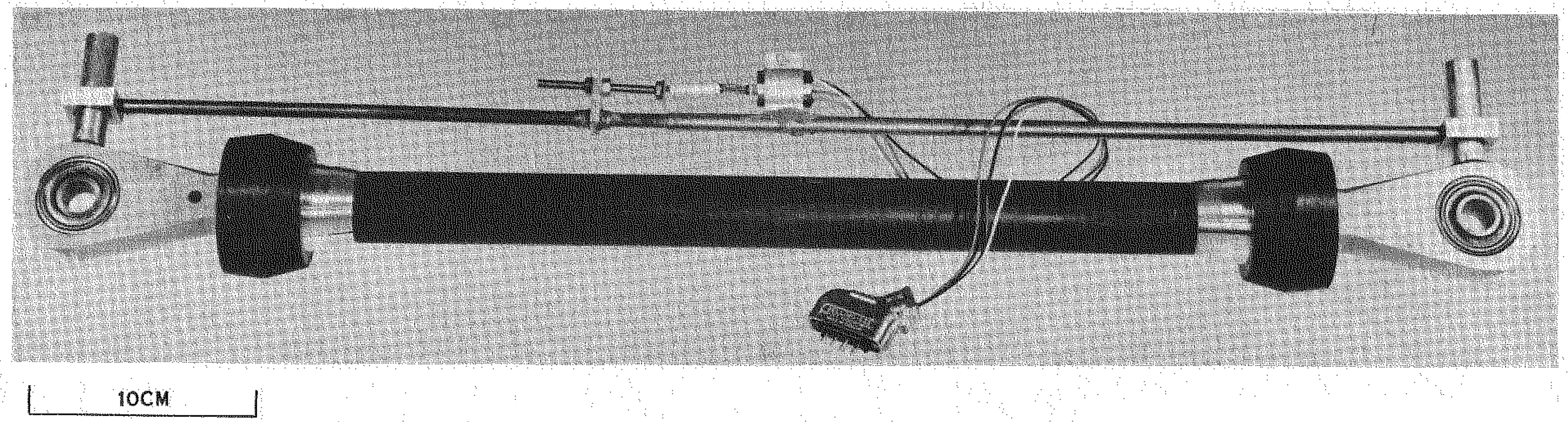

Fig.36   Instrumentation for stiffness measurement

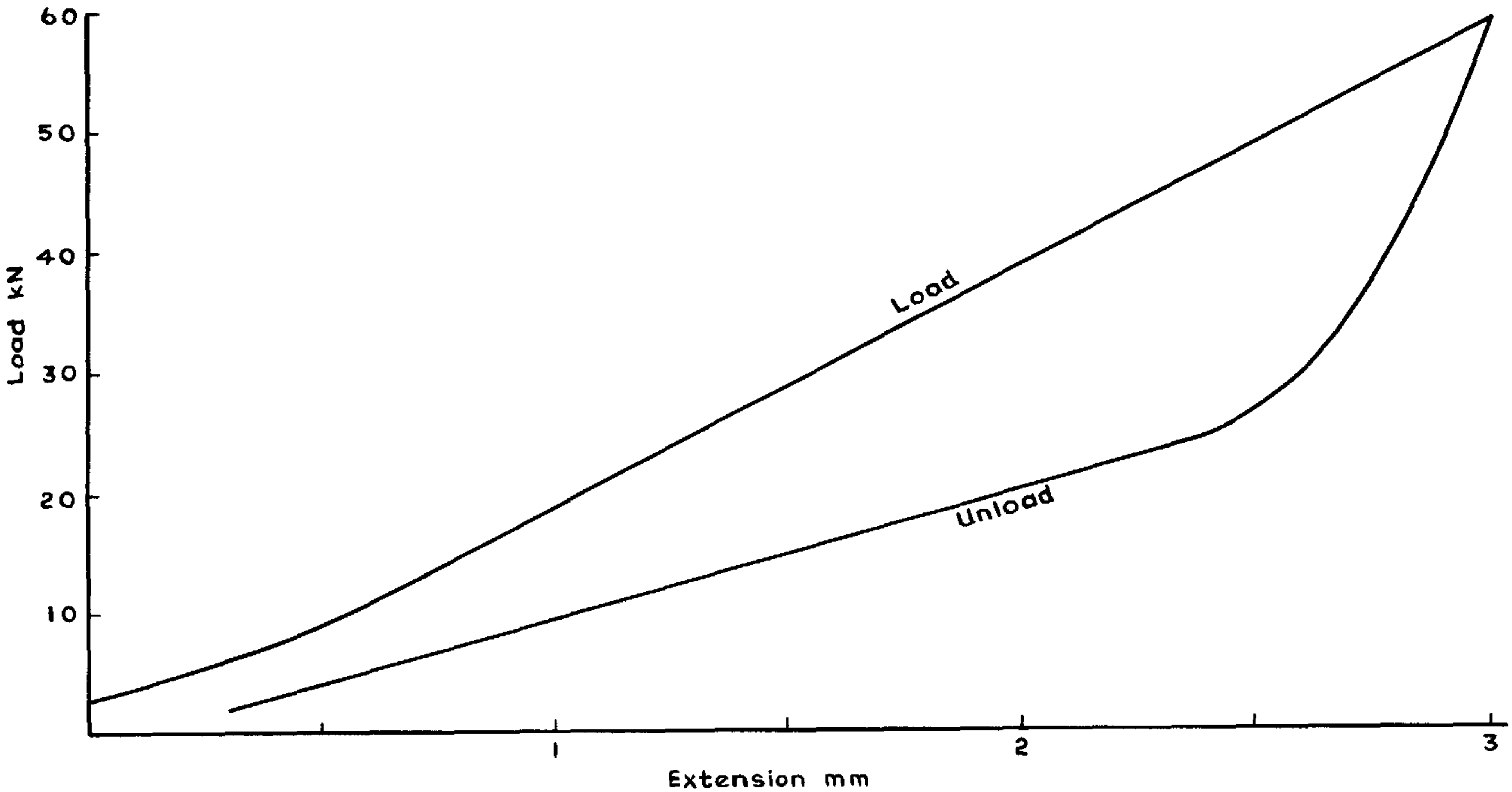

Fig.37 Variation of extension with load for strut assembly loaded in tension

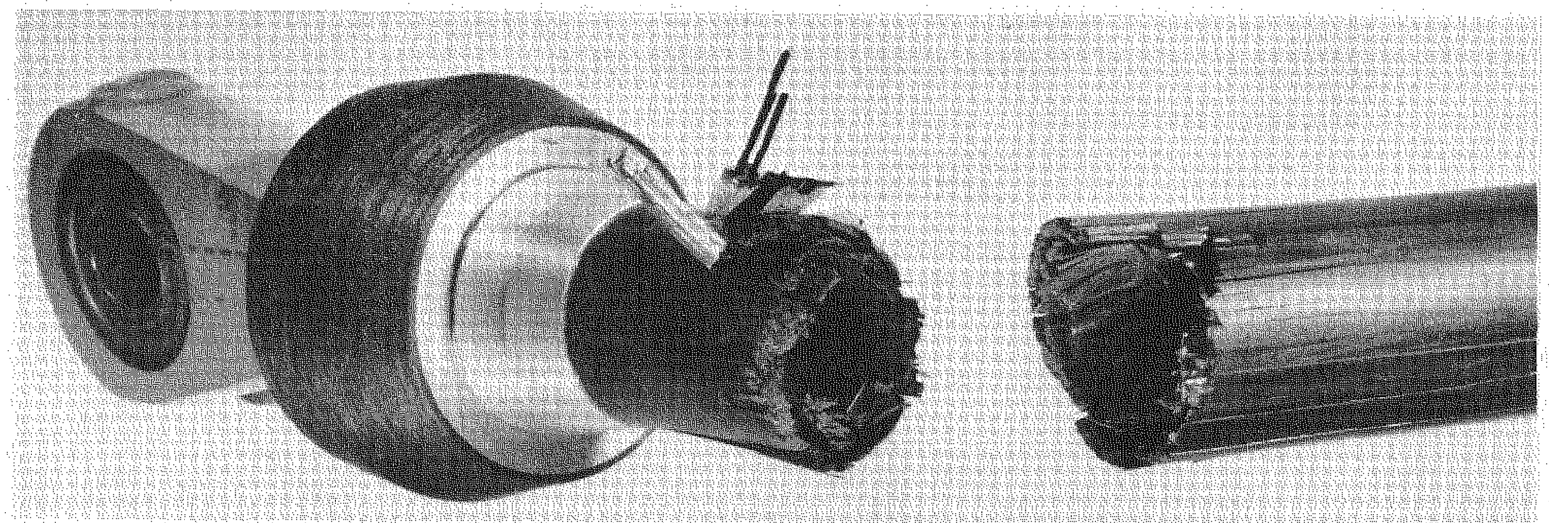

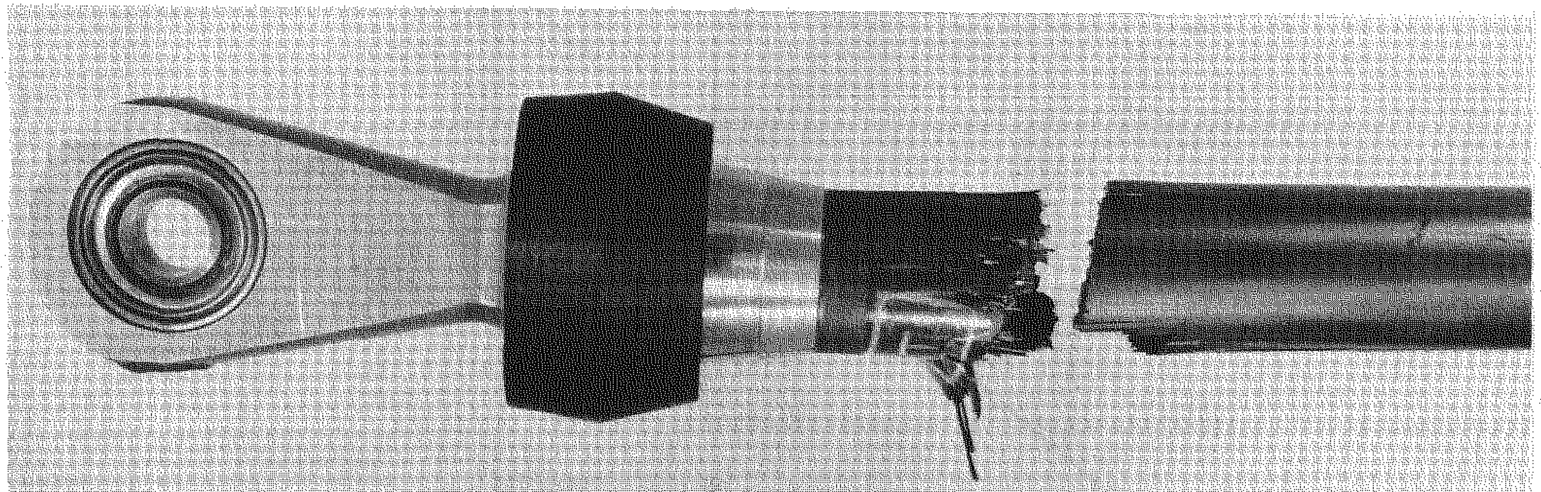

Fig.38 Compression test failure strut model 4

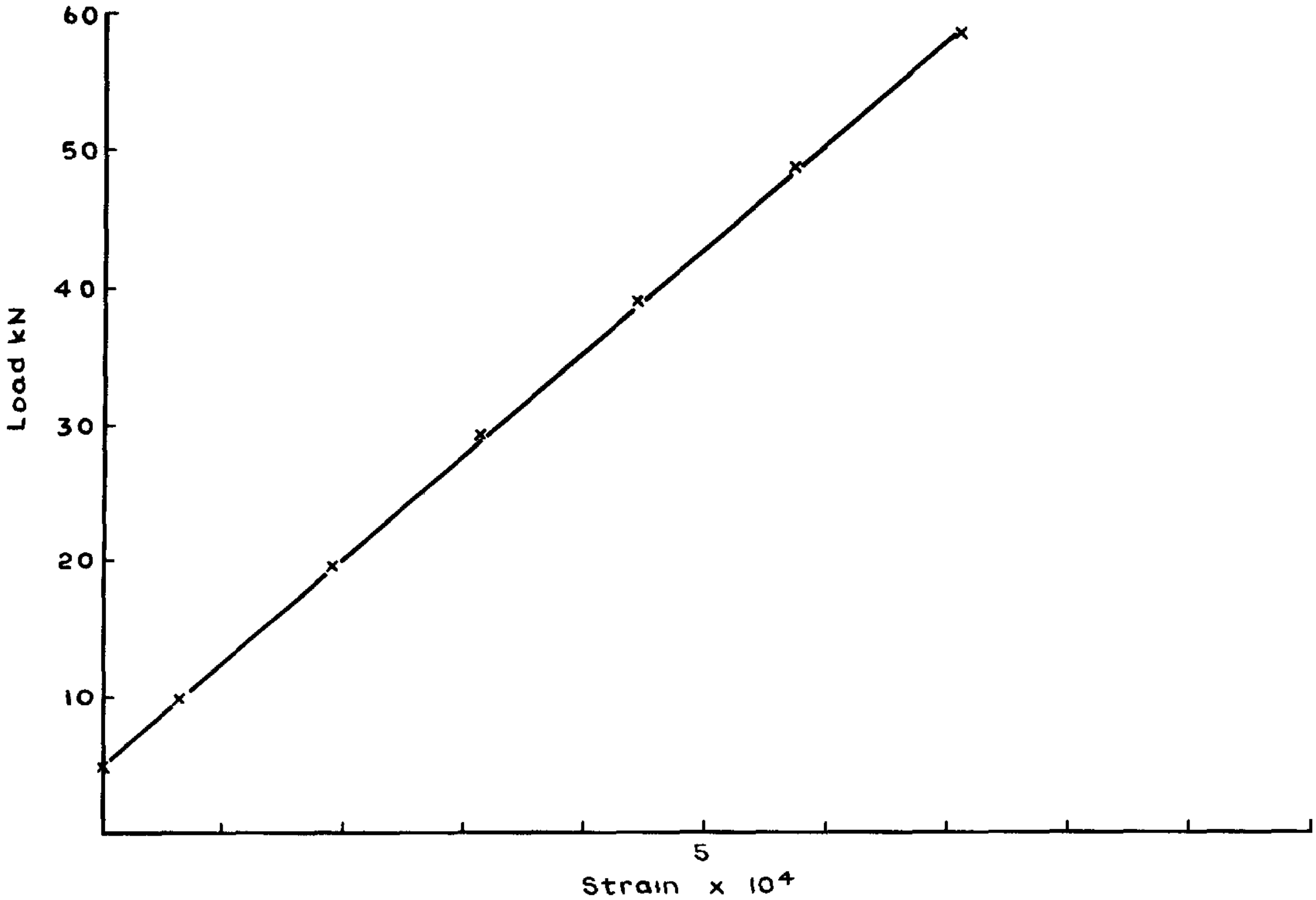

Fig. 39 Variation of strain with load for CFRP tube loaded in compression

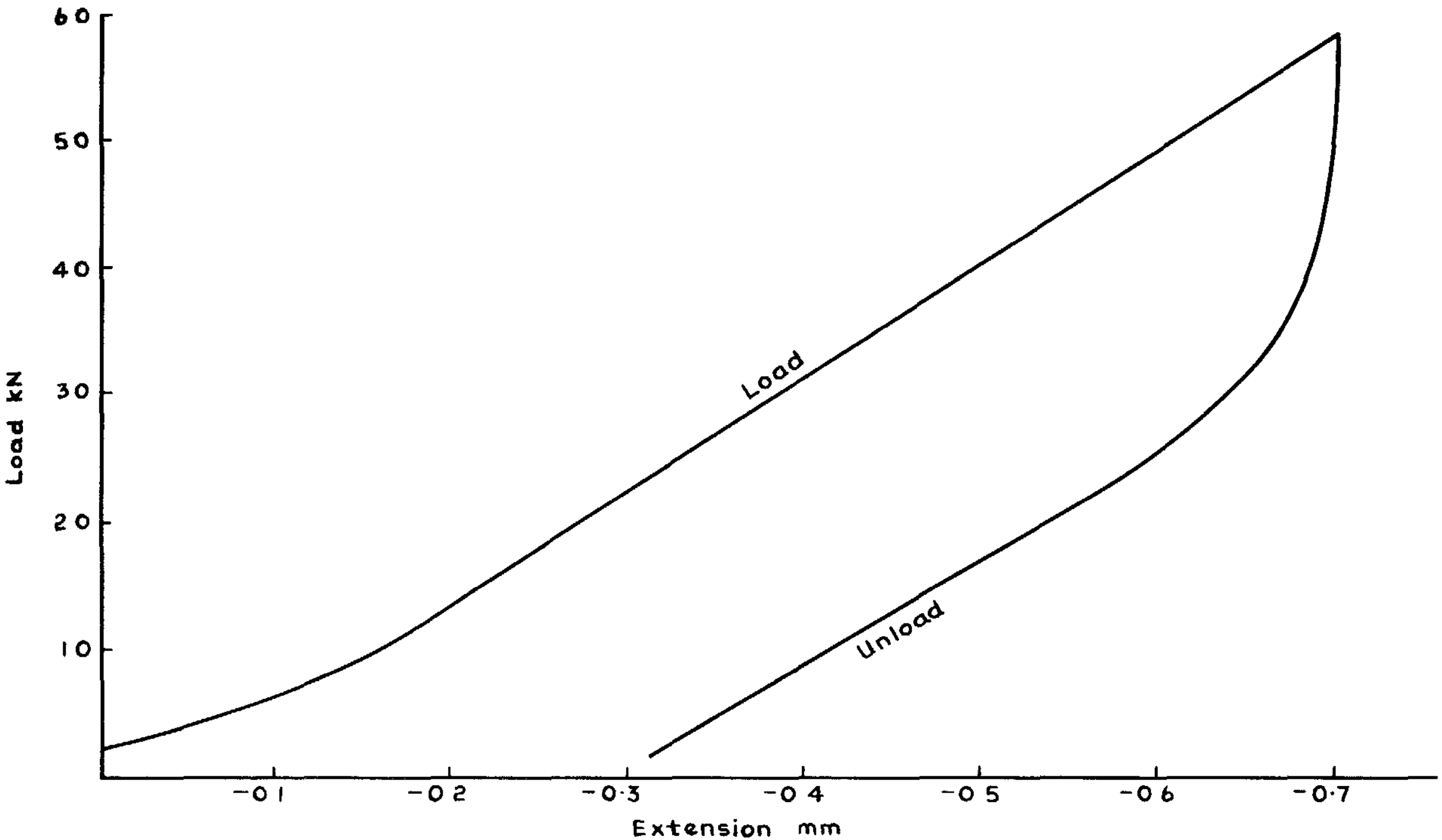

Fig. 40 Variation of extension (-ve) with load for strut assembly loaded in compression

Printed in England for Her Majesty's Stationery Office by the Royal Aircraft Establishment, Farnborough Dd 503427 K 4 8/72

ARC CP No 1229
February 1972

Collings, T A

629.13 012 563
621-23
661.66-426
678 046

DESIGN DEVELOPMENT OF AN AIRCRAFT STRUT
IN CARBON FIBRE REINFORCED PLASTIC

An actuator reaction strut from the VC 10 aileron power control circuit, made from steel, has been redesigned, made and tested in carbon fibre reinforced plastic (CFRP) with aluminium alloy ends, partly to demonstrate the weight saving potential of CFRP in this type of application and partly to investigate some of the problems of jointing and load diffusion which CFRP presents

The strut has overall axial strength and stiffness requirements in both tension and compression All have been met with the redesigned CFRP strut with the exception of tensile stiffness, the low value of which was shown to be fundamental to the form of end attachment adopted

This Report describes the design, fabrication and testing of the CFRP strut which weighed 43% less than the original steel component

These abstract cards are inserted in Technical Reports for the convenience of Librarians and others who need to maintain an Information Index

Detached cards are subject to the same Security Regulations as the parent document, and a record of their location should be made on the inside of the back cover of the parent document

Cut here

ARC CP No 1229
February 1972

Collings, T A

629 13 012 563
621-23
661 66-426
678 046

DESIGN DEVELOPMENT OF AN AIRCRAFT STRUT
IN CARBON FIBRE REINFORCED PLASTIC

An actuator reaction strut from the VC 10 aileron power control circuit, made from steel, has been redesigned, made and tested in carbon fibre reinforced plastic (CFRP) with aluminium alloy ends, partly to demonstrate the weight saving potential of CFRP in this type of application and partly to investigate some of the problems of jointing and load diffusion which CFRP presents

The strut has overall axial strength and stiffness requirements in both tension and compression All have been met with the redesigned CFRP strut with the exception of tensile stiffness, the low value of which was shown to be fundamental to the form of end attachment adopted

This Report describes the design, fabrication and testing of the CFRP strut which weighed 43% less than the original steel component

ARC CP No 1229
February 1972

Collings, T A

629 13 012 563
621-23
661 66-426
678 046

DESIGN DEVELOPMENT OF AN AIRCRAFT STRUT
IN CARBON FIBRE REINFORCED PLASTIC

An actuator reaction strut from the VC 10 aileron power control circuit, made from steel, has been redesigned, made and tested in carbon fibre reinforced plastic (CFRP) with aluminium alloy ends, partly to demonstrate the weight saving potential of CFRP in this type of application and partly to investigate some of the problems of jointing and load diffusion which CFRP presents

The strut has overall axial strength and stiffness requirements in both tension and compression All have been met with the redesigned CFRP strut with the exception of tensile stiffness, the low value of which was shown to be fundamental to the form of end attachment adopted

This Report describes the design, fabrication and testing of the CFRP strut which weighed 43% less than the original steel component

Cut here

DETACHABLE ABSTRACT CARDS

DETACHABLE ABSTRACT CARDS

C.P. No. 1229

Published by
HER MAJESTY'S STATIONERY OFFICE

To be purchased from
49 High Holborn, London WC1 V 6HB
13a Castle Street, Edinburgh EH2 3AR
109 St Mary Street, Cardiff CF1 1JW
Brazennose Street, Manchester M60 8AS
50 Fairfax Street, Bristol BS1 3DE
258 Broad Street, Birmingham B1 2HE
80 Chichester Street, Belfast BT1 4JY
or through booksellers

C.P. No. 1229

SBN 11 470787 1